

Thermalization of mini-jets in a quark-gluon plasma

Edmond Iancu and Bin Wu

Institut de Physique Théorique, CEA Saclay, UMR 3681, F-91191 Gif-sur-Yvette, France

E-mail: Edmond.Iancu@cea.fr, Bin.Wu@cea.fr

ABSTRACT: We complete the physical picture for the evolution of a high-energy jet propagating through a weakly-coupled quark-gluon plasma by investigating the thermalization of the soft components of the jet. We argue that the following scenario should hold: the leading particle emits a significant number of mini-jets which promptly evolve via quasi-democratic branchings and thus degrade into a myriad of soft gluons, with energies of the order of the medium temperature T . Via elastic collisions with the medium constituents, these soft gluons relax to local thermal equilibrium with the plasma over a time scale which is considerably shorter than the typical lifetime of the mini-jet. The thermalized gluons form a tail which lags behind the hard components of the jet. We support this scenario, first, via parametric arguments and, next, by studying a simplified kinetic equation, which describes the jet dynamics in longitudinal phase-space. We solve the kinetic equation using both (semi-)analytical and numerical methods. In particular, we obtain the first exact, analytic, solutions to the ultrarelativistic Fokker-Planck equation in one-dimensional phase-space. Our results confirm the physical picture aforementioned and demonstrate the quenching of the jet via multiple branching followed by the thermalization of the soft gluons in the cascades.

KEYWORDS: Perturbative QCD. Heavy Ion Collisions. Jet quenching. Wave turbulence

Contents

1	Introduction	1
2	The physical picture	5
2.1	Multiple branching and the medium-induced gluon cascade	6
2.2	Elastic collisions and thermalization	10
3	The kinetic equation for the longitudinal dynamics	13
4	Semi-analytic studies of the kinetic equation	17
4.1	Thermalization for a steady source	18
4.2	Jet quenching in the source approximation	21
4.2.1	The Fokker-Planck Green’s function	21
4.2.2	A physical source generated by the branching process	25
5	Numerical studies of the kinetic equation	27
5.1	Setting-up the problem	28
5.2	The gluon spectrum	29
5.3	Jet evolution in longitudinal phase-space	31
5.3.1	The gluon distribution and the energy density	31
5.3.2	Energy loss towards the medium	36
6	Conclusions and perspectives	38

1 Introduction

It is by now well established that, within weakly-coupled QCD at least, the energy loss by an energetic parton and/or the associated jet propagating through a dense medium, such as a quark-gluon plasma, is dominated by *medium-induced radiation*, that is, the additional radiation triggered by the interactions between the partons from the jet and the medium constituents [1–11] (see also the review papers [12–14]). This picture has led to a rather successful phenomenology, based on, or at least inspired by, calculations in perturbative QCD, which has allowed one to understand many interesting observables at RHIC and the LHC, like the nuclear modification factor or the suppression of di-hadron azimuthal correlations in ultrarelativistic nucleus-nucleus collisions [15–18].

More recently, the experimental studies of the phenomenon known as ‘di-jet asymmetry’ in Pb+Pb collisions at the LHC have demonstrated that a substantial fraction of the energy loss by an energetic jet is carried by relatively soft hadrons propagating at large angles with respect to the jet axis [19–26]. This pattern too can be understood, at least qualitatively, within the pQCD picture for medium-induced radiation, which predicts the formation of well-developed gluon cascades, or ‘mini-jets’, via multiple branching [27–35] (see also Refs. [36–39] for earlier, related, studies and the recent review

paper [40]). Within these cascades, the energy is efficiently transmitted, via quasi-democratic branchings, from the ‘leading particle’ — the parton that has initiated the (mini)jet — to a large number of comparatively soft gluons, which can be easily deviated towards large angles by rescattering in the medium. The theoretical description of medium-induced multiple branching started being developed only recently and in its current formulation it leaves unanswered a number of important questions.

The basic question is, what is the microscopic mechanism responsible for the energy loss? Of course, one already knows that, from the perspective of the leading particle, the dominant mechanism at work is radiative energy loss and that the energy carried by the primary radiation is efficiently transmitted to softer and softer particles, via successive branchings in the gluon cascades. But what is the physical mechanism which *stops* these cascades, and at which energy scale (i.e., what is the *low-energy end* of the cascade)? How does this mechanism influence the dynamics of the branchings at *higher* energy scales? And *where* does the energy go, when it flows out of the cascade?

In order to better appreciate these questions, it is useful to briefly recall our current understanding of the medium-induced jet evolution via multiple branching (see Sect. 2 below for details). The gluon cascades which are relevant for us here are those generated by iterating gluon emissions of the BDMPSZ type¹ [2–5]. The BDMPSZ mechanism governs the emission of relatively hard gluons, with energies $\omega \gg T$, which undergo multiple scattering in the surrounding medium. Here, T is the characteristic energy scale of the medium, say, the temperature for the case of a quark-gluon plasma in thermal equilibrium, or, more generally, the average p_T of the background hadrons. The distinguished feature of this mechanism for our present purposes is the fact that it favors ‘quasi-democratic branchings’, that is, $1 \rightarrow 2$ gluon splittings where the daughter gluons carry comparable fractions of the energy of their parent gluon. Such branchings occur fast and are extremely efficient in redistributing the energy among the branching products: they lead to turbulent cascades, in which the energy flows from one parton generation to the next one, without accumulating at intermediate steps.

In most theoretical analyses so far, one has assumed, for simplicity, that the branching dynamics remains unmodified down to arbitrarily low energies. This allowed for elegant and physically transparent solutions [28, 30, 35], which exhibit *wave turbulence* with a characteristic scaling spectrum — the analog of the Kolmogorov–Zakharov spectrum [41, 42] for the medium-induced cascades — and have interesting consequences for the energy loss by the jet (see Sect. 2 below). But such an ‘ideal’ cascade leads also to unphysical results: after a finite interval of time (the ‘branching time’ $t_{\text{br}}(E)$, to be specified in Sect. 2) the original energy E of the leading particle gets transmitted to quanta which are arbitrarily soft ($\omega \rightarrow 0$) and hence can propagate at arbitrarily large angles. While this peculiar ‘final state’ is clearly unacceptable, it is important to stress that the phenomenon of wave turbulence is in fact more general and could very well coexist with a physically acceptable final state: the scaling spectrum survives unchanged if one stops the branching process at some finite energy scale $p_* \ll E$, by introducing there a ‘perfect sink’. The ‘perfect sink’ — a concept familiar in the theory of turbulence [41, 42] — is, by definition, a mechanism which is capable to absorb the energy flux generated by the cascade at p_* , without influencing the branching dynamics at higher energies $\omega \gg p_*$.

On physical grounds, there is an obvious candidate for such a ‘sink’: the surrounding medium. The soft gluons from the cascade with $\omega \sim T$ are expected to thermalize via collisions in the medium and thus deposit their energy inside the medium. This motivated proposals in the literature to terminate the cascade at the medium scale T , e.g. by enforcing an ‘infrared’ cutoff $p_* \sim T$ on the

¹The acronym ‘BDMPSZ’ stands for Baier, Dokshitzer, Mueller, Peigné, Schiff, and Zakharov.

branching dynamics [30, 32]. But such previous arguments were insufficiently developed; it was not clear, e.g., what is the actual thermalization mechanism, why should this inhibit the branching process, and whether this should act as a ‘perfect sink’, or, on the contrary, wash out the wave turbulence. [Numerical simulations using an ad-hoc infrared cutoff p_* [32] observed a strong distortion of the scaling spectrum, due to the accumulation of gluons in the bins above p_* . With increasing time, this pile-up extends up to high energies $\omega \gg p_*$ (see also the discussion in Sect. 5.2 below).]

It is our main purpose in this paper to clarify these and related questions, via a dedicated theoretical analysis. Specifically, assuming the medium to be a weakly-coupled quark-gluon plasma with temperature T , we shall study the possibility that the soft components of the jet, with energies $\omega \sim T$, thermalize via elastic constituents with the quarks and gluons from the plasma. To that aim, we shall consider a special kinetic equation, which emerges via specific approximations from more general (but also more difficult to solve) equations existing in the literature [36, 43], and which will be argued to capture the interesting dynamics to parametric accuracy at least. This equation, to be introduced in Sect. 3, describes the evolution of the gluon distribution $f(t, z, p_z)$ created by the jet in the longitudinal phase-space, with the z axis referring to the direction of propagation of the leading particle.

The kinetic equation includes two types of collision terms: an inelastic one, describing multiple branching with the BDMPSZ splitting rate, and an elastic one, which describes $2 \rightarrow 2$ collisions with the medium constituents in the Fokker-Planck approximation [44]. The latter is *a priori* suitable for a probe particle, or a dilute system of such particles, which can be distinguished from the thermal bath (like a heavy quark [45, 46]), but can also be applied to the gluons from the jet with relatively large momenta $p_z \simeq \omega \gg T$ [47]. Indeed, the occupation numbers for the gluons generated via multiple branching remain very small down to $\omega = T$, as we shall see (cf. the discussion in Sect. 2.1).

We shall further argue that, as a result of thermalization, the branching process effectively terminates at the medium scale $\omega \sim T$ and we shall mimic this by inserting an ‘infrared’ cutoff $p_* \sim T$ in the splitting rate. The physical mechanism beyond this cutoff will be clarified too — this is related to the non-linear effects in the *total* gluon distribution, i.e. the distribution produced by the medium plus the jet (see the discussion in Sect. 3) —, but a proper treatment of this mechanism would require working with the non-linear kinetic equation obeyed by the full distribution, a task which is extremely hard in practice. As we shall see in our numerical simulations, the physics around this cutoff is smeared by elastic collisions and thermalization, so in practice we do not expect strong artifacts related to p_* .

Finally, the restriction to the longitudinal dynamics is needed to simplify the problem (in particular, in view of numerical calculations) but it is also physically motivated. The longitudinal momenta remain much larger than the respective transverse components ($p_z \gg p_\perp$) so long as $\omega \gg T$, that is, during most stages of the dynamics, where they control the relevant time scales. This approximation fails, strictly speaking, in the approach towards thermal equilibrium, but even in that case it captures the correct time dependence to parametric accuracy. (In fact, a similar approximation has been used in all the previous studies of the in-medium cascade, including those which have explicitly considered the dependence upon transverse momenta [29, 31, 32, 34].) Furthermore, the gluon distribution along the longitudinal axis z is the most interesting one in view of a study of thermalization, since this is strongly inhomogeneous to start with: in the absence of collisions, all the gluons in the jet, even the softest ones, would propagate along the light-cone at $z = t$, together with the leading particle.

In view of the above approximations, we expect that a thermalized distribution emerging from our kinetic equation should look like a ‘tail’ lying well behind the front of the jet, i.e. at $|z| \ll t$, where it is quasi-homogeneous, and which in longitudinal momentum features the classical thermal distribution

for massless particles in one spatial dimension, that is, the Maxwell-Boltzmann distribution $e^{-|p_z|/T}$. This is indeed what we shall observe in our solutions.

Specifically, we shall study the kinetic equation via a combination of (semi)analytic and numerical methods. For the Fokker-Planck dynamics alone, we will be able to find exact, analytic, solutions — in particular, the solution corresponding to a steady source along the light-cone (in Sect. 4.1) and the exact Green’s function in longitudinal phase-space (see Sect. 4.2.1). To our knowledge, these are the first examples of exact solutions for a relativistic Fokker-Planck equation. By combining this Green’s function with known, analytic, solutions for the (ideal) branching process [28, 30, 35], we have been able to give a relatively simple, semi-analytic, analysis of the full dynamics, under the assumption that the medium acts as a perfect sink at the scale $p_* = T$. (Under this assumption, it is indeed well justified to treat the branching part of the dynamics as a source which injects gluons at the scale p_* at a rate known from the previous analyses of the turbulent cascade; see the discussion in Sect. 4.)

In order to test the ‘perfect sink’ assumption and also to have more a complete study which includes the interplay between branchings and elastic collisions at energies $\omega > p_*$, we present in Sect. 5 a detailed numerical analysis of the kinetic equation, with infrared cutoff $p_* = T$ in the branching integral. The numerical solutions turn out to be qualitatively similar to the semi-analytic ones in Sect. 4, but they bring additional clarifications, in particular, on the role of the infrared cutoff p_* and, related to that, on the limitations of the ‘perfect sink’ approximation.

The overall physical scenario which emerges from these explicit solutions is in agreement with the general picture anticipated in Sect. 2, but it is more precise and also more complete than the latter. It can be summarized as follows (see Sects. 2 and 5 for details):

A ‘leading particle’ (LP) with initial energy $E \gg T$ which crosses the medium along a distance L radiates abundantly (i.e., with a probability of order one) relatively soft gluons with energies $\omega \lesssim \omega_{\text{br}}(L)$. Here, $\omega_{\text{br}}(L) \sim \alpha_s^2 \hat{q} L^2$, with $\hat{q} \sim \alpha_s^2 T^3 \ln(1/\alpha_s)$ the jet quenching parameter, is the characteristic energy scale for democratic branchings: gluons with smaller energies $\omega \lesssim \omega_{\text{br}}(L)$ can undergo a democratic branching within a time $\Delta t \lesssim L$, where those with higher energies $\omega \gg \omega_{\text{br}}(L)$ cannot. In the experimental conditions at the LHC, one typically has $T \ll \omega_{\text{br}}(L) \ll E$, so the LP belongs to the second category above, whereas the ‘primary gluons’ emitted by it belong to the first one. Accordingly, each of these ‘primary gluons’ generates a gluon cascade (‘mini-jet’) via successive democratic branchings. Each such a cascade ends at the thermal scale T , meaning that the energy ω of a primary gluon gets distributed among a large number $\omega/T \gg 1$ of soft gluons. These gluons undergo elastic collisions with the medium constituents and thus relax to a thermal distribution in momentum after a time of order $t_{\text{rel}} \sim T^2/\hat{q}$. At the same time they separate in z from the harder partons (which keep propagating along the light-cone) and thus form a tail at $|z| < t$, which lags behind the front. Therefore the momentum distribution looks very different near the front of the jet ($z \simeq t$), where the spectrum shows an approximate scaling behavior, as expected for ‘ideal’ branching, and in the tail at $z < t$, where the distribution is nearly thermal.

The energy carried away by the gluons in the thermalized tail is naturally interpreted as the *energy lost by the jet to the medium*. This is controlled by the hardest ‘mini-jets’, those with energies $\omega \sim \omega_{\text{br}}(L)$, and therefore it scales with the medium size like L^2 . More precisely, the L^2 -scaling is the respective prediction of the ideal branching process, where the energy loss is computed as the energy carried by the turbulent flow [28, 30]. For the full dynamics including elastic collisions and thermalization, we numerically find that the energy deposited by the jet inside the medium is somewhat smaller than this ‘ideal’ prediction, albeit comparable to it. This reduction reflects the fact

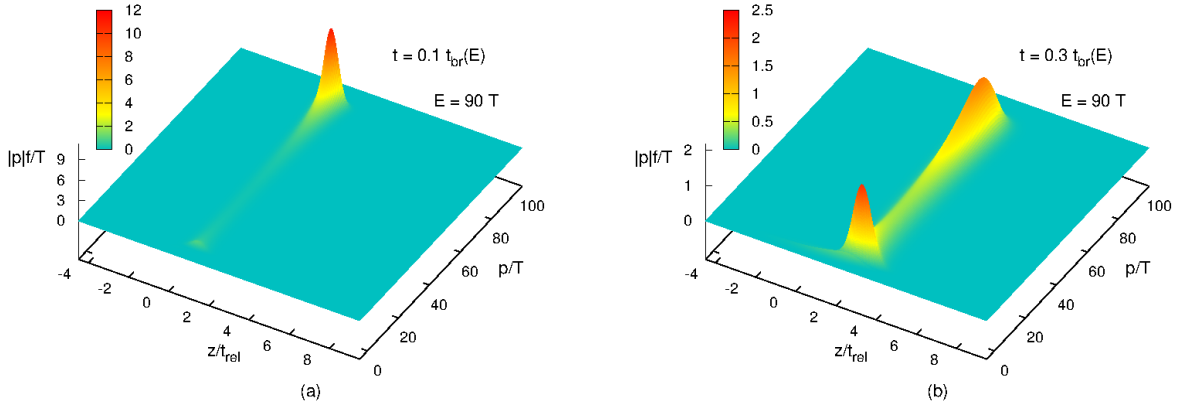


Figure 1. The phase-space energy density $|p|f/T$ produced by an energetic jet with $E = 90 T$ at two successive times: (a) an early time $t = 0.1 t_{\text{br}}(E)$, when the jet is almost unquenched; (b) a larger time $t = 0.3 t_{\text{br}}(E)$, when the jet is partially quenched. The secondary peak visible around $p \sim T$ in plot (b) represents the energy lost towards the medium via thermalization. The reference scale $t_{\text{br}}(E)$ is the characteristic time scale for the evolution of the jet via democratic branching, to be explained in Sect. 2.1 (this is given by Eq. (2.5)).

that the medium is not a ‘perfect sink’, more precisely the fact that the soft gluons cannot thermalize *instantaneously* (see the discussion in Sect. 5.3.2).

The above considerations are illustrated by the plots in Fig. 1 which are in fact extracted from our numerical results in Sect. 5. These plots show the (normalized) energy distribution $(|p|/T)f(t, z, p)$ (with $p \equiv p_z$) produced by an incoming leading particle with $E = 90 T$ at two successive times, an early time, when the jet is almost unquenched, and a later time, when the jet is partially quenched. In the ‘late time’ plot in Fig. 1 (b), one clearly sees the accumulation of particles at soft momenta $p \lesssim T$, due to branchings and elastic collisions.

Let us finally stress that the above picture strictly holds for a very energetic jet, with initial energy $E \gg \omega_{\text{br}}(L)$, which is only ‘slightly quenched’ — meaning that the LP survives in the final state and the energy lost towards the medium is only a small fraction of the initial energy E . In that case, the final distribution, as visible in Fig. 1 (b), may be viewed as the superposition of the LP peak together with the distributions separately created by all the ‘mini-jets’. But the individual ‘mini-jets’ have lower energies $\omega \lesssim \omega_{\text{br}}(L)$, so they are fully quenched by the medium — their whole energy gets transmitted to the thermalized tail and the mini-jets disappear in the medium. The distribution created by a single mini-jet will be discussed too in Sect. 5.

2 The physical picture

In this section, we summarize the physical picture underlying the in-medium evolution of a jet generated by a high-energy parton propagating through a weakly-coupled quark-gluon plasma. This picture largely reflects the current understanding of this problem, as emerging from the literature, but includes some additional arguments which will be physically motivated, together with some expectations to be subsequently confirmed by the new analysis in this work. We start with a brief review of recent studies of the medium-induced gluon cascade [27–30], which recognized the importance of multiple

branchings, but did not address the important problem of the thermalization of the soft components of the jet. Then we discuss the interplay between multiple branching and the elastic collisions responsible for thermalization.

2.1 Multiple branching and the medium-induced gluon cascade

An energetic ‘probe’ parton (gluon or quark) which propagates through a dense QCD medium, such as a quark-gluon plasma, undergoes elastic collisions with the constituents of the medium, leading to ‘collisional’ energy loss — on the average, the energy transferred from the probe to the medium is larger than in the opposite direction — and to the broadening of the probe distribution in (longitudinal and transverse) momentum, due to the random nature of the ‘kicks’. Besides, the collisions trigger gluon emissions by the probe, leading to additional, ‘radiative’, energy loss, which in practice dominates over the collisional one, in spite of the fact that the emission probability is suppressed by a factor of α_s . This is possible because the coherence effects inherent in a quantum emission lead to a stronger dependence of the energy loss upon the medium size — the radiative component rises, roughly, like L^2 (with L the distance traveled by the probe through the medium), whereas the collisional component rises only like L . Notwithstanding, the elastic collisions will play an important role for the subsequent discussion — as we shall see, it is responsible for the in-medium deposition of the energy lost via radiation in a typical event.

The precise mechanism responsible for medium-induced radiation depends upon the ratio between the gluon ‘formation time’ $t_{\text{form}} \sim \omega/p_{\perp}^2$ (the typical duration of the emission, as fixed by the uncertainty principle) and the mean free path $\lambda_{\text{mfp}} \sim 1/[\alpha_s T \ln(1/\alpha_s)]$ between two successive small-angle collisions. Here, ω is the energy of the emitted gluon and p_{\perp} is its transverse momentum, as acquired during the formation time, via collisions. For a single collision, one typically has $p_{\perp}^2 \sim m_D^2 \sim \alpha_s T^2$, with m_D the Debye mass. For a series of independent collisions occurring during a time interval $\Delta t \gg \lambda_{\text{mfp}}$, one has $p_{\perp}^2 \sim \hat{q} \Delta t$, where $\hat{q} \simeq m_D^2/\lambda_{\text{mfp}} \sim \alpha^2 T^3 \ln(1/\alpha_s)$ is the ‘jet quenching parameter’ — a transport coefficient which characterizes momentum diffusion. Using these estimates, one finds that, with increasing ω , one interpolates between a single-scattering (or ‘Bethe-Heitler’) regime at low energies $\omega \lesssim T$, where $t_{\text{form}} \sim \omega/m_D^2 \lesssim \lambda_{\text{mfp}}$, and a multiple-scattering (or ‘LPM’, from Landau, Pomeranchuk, and Migdal) regime at high energies $\omega \gg T$, where $t_{\text{form}} \sim \sqrt{\omega/\hat{q}} \gg \lambda_{\text{mfp}}$. In the LPM regime, there is a large number of collisions which coherently contribute to a single emission.

In what follows, we shall consider the LPM regime alone. Indeed, we shall later argue that the branching process terminates around $\omega \sim T$, hence the phase-space for Bethe-Heitler radiation is comparatively small. The calculation of the gluon branching rate in the LPM regime to leading order in pQCD has been first given by Baier, Dokshitzer, Mueller, Peigné, and Schiff [2, 3, 6], and independently by Zakharov [4, 5]. One has thus obtained the following result for the differential probability per unit time and per unit x for the collinear splitting² of a gluon with energy ω into two daughter gluons with energy fractions x and $1 - x$, with $0 < x < 1$:

$$\frac{d^2 \mathcal{I}_{\text{br}}}{dx dt} = \frac{\alpha_s}{2\pi} \frac{P_{g \rightarrow g}(x)}{t_{\text{form}}(x, \omega)}. \quad (2.1)$$

²The splitting is effectively collinear since the transverse momentum squared acquired by the gluon during the formation time t_{form} is much smaller than the respective quantity acquired after formation, namely during the lifetime $t_{\text{br}} \sim t_{\text{form}}/\bar{\alpha}$ of the gluon until its next splitting (see below).

In this equation, $P_{g \rightarrow g}(x) = N_c [1 - x(1 - x)]^2 / x(1 - x)$, with N_c the number of colors, is the leading order gluon–gluon splitting function of the DGLAP equation and $t_{\text{form}}(x, \omega)$ is a more precise estimate for the formation time, which involves the average energy $x(1 - x)\omega$ of the two daughter gluons:

$$t_{\text{form}}(x, \omega) \equiv \sqrt{\frac{x(1 - x)\omega}{\hat{q}_{\text{eff}}(x)}}, \quad \hat{q}_{\text{eff}}(x) \equiv \hat{q} [1 - x(1 - x)]. \quad (2.2)$$

Using Eq. (2.1), one can evaluate the probability for a branching to occur during a given interval Δt :

$$\Delta \mathcal{P} \simeq x \frac{d^2 \mathcal{I}_{\text{br}}}{dx dt} \Delta t \sim \bar{\alpha} \sqrt{\frac{\hat{q}}{x(1 - x)\omega}} \Delta t, \quad (2.3)$$

where $\bar{\alpha} \equiv \alpha_s N_c / \pi$. This probability becomes of order one, meaning that multiple branching is important during Δt , provided

$$x(1 - x)\omega \sim \bar{\alpha}^2 \hat{q} \Delta t^2 \equiv \omega_{\text{br}}(\Delta t). \quad (2.4)$$

This condition can be satisfied by two types of emissions:

(a) very asymmetric splittings, for which either $x \ll 1$ or $1 - x \ll 1$, whereas the energy ω of the parent gluon can be relatively hard (for instance, $\omega \gg \omega_{\text{br}}(\Delta t)$);

(b) ‘quasi-democratic’ branchings, where the two daughter gluons carry comparable fractions of the total energy, $x \sim 1 - x \sim \mathcal{O}(1)$, but the parent gluon is relatively soft: $\omega \sim \omega_{\text{br}}(\Delta t)$.

Reversing the argument for case (b) above, we conclude that it takes a time $\Delta t \sim t_{\text{br}}(\omega)$, with

$$t_{\text{br}}(\omega) \equiv \frac{1}{\bar{\alpha}} \sqrt{\frac{\omega}{\hat{q}}}, \quad (2.5)$$

for a gluon with energy ω to undergo a ‘quasi-democratic’ branching [28, 36, 48]. This duration $t_{\text{br}}(\omega)$ should be compared to the medium size L which is available to that parton:

(i) If $t_{\text{br}}(\omega) \gg L$, then the parton with energy ω can emit *abundantly* — i.e. with probability of $\mathcal{O}(1)$ — only relatively soft gluons with $x \ll 1$, in such a way that $x\omega \lesssim \omega_{\text{br}}(L) = \bar{\alpha}^2 \hat{q} L^2$. Accordingly, the original parton will ‘survive the medium’: it will be recognizable in the final state due to the fact that its final energy will be considerably higher than for all the other gluons, as produced by radiation.

(ii) If $t_{\text{br}}(\omega) \lesssim L$, then the parton with energy ω will ‘disappear inside the medium’ — it will undergo a quasi-democratic branching before it exits the medium and thus it will be replaced by a pair of softer gluons, which can ‘democratically’ split again. Eventually, the original parton will leave behind it a gluon cascade generated via successive, quasi-democratic splittings. Note that each new gluon generation in that cascade has a lower energy and hence a shorter lifetime than the previous ones. Accordingly, the overall lifetime of the cascade is of the order of the branching time $t_{\text{br}}(\omega)$ of the initial gluon.

Case (i) is the interesting situation for the leading particle (LP) which initiates a typical jet measured in Pb+Pb collisions at the LHC. Indeed, denoting the energy of this LP by E , one generally has $E \geq 100$ GeV, whereas the characteristic energy for multiple branching is much smaller: $\omega_{\text{br}}(L) = \bar{\alpha}^2 \hat{q} L^2 \simeq 12$ GeV for a medium with $\hat{q} = 1$ GeV²/fm and $L = 5$ fm (we used $\bar{\alpha} = 0.3$). The above estimate also shows that, for the interesting values of L , the branching scale $\omega_{\text{br}}(L)$ is much harder than the medium temperature $T \simeq 0.5$ GeV; hence, one typically has $T \ll \omega_{\text{br}}(L) \ll E$.

Case (ii) applies to the *typical* primary gluons — the gluons which are directly radiated by the LP in a typical event —, which have relatively soft energies $\omega \lesssim \omega_{\text{br}}(L)$ and thus have the time to develop gluon cascades (‘mini-jets’) via quasi-democratic branchings. Harder primary emissions, with energies up to³ $\omega_c \equiv \hat{q}L^2$, are possible as well (provided $E > \omega_c$, of course), but these are rare events which occur with a probability of $\mathcal{O}(\bar{\alpha})$ and do not generate mini-jets. Such hard but rare emissions will not be explicitly considered in what follows, since they do not contribute to the energy loss by the jet towards the medium. (But they are important for the average energy loss by the LP [2–6].)

The quasi-democratic nature of the splittings has important consequences for the energy flow across a mini-jet: it leads to *wave turbulence* [28, 30]. Via successive branchings, the energy flows from one gluon generation to the next one, without accumulating at any intermediate value of ω . The precise mathematical condition for wave turbulence is that the energy flux — the rate for energy flow along the cascade — should be independent of ω . This condition is indeed satisfied for the gluon cascade generated by a primary gluon with energy $\omega_0 \lesssim \omega_{\text{br}}(L)$, at least at sufficiently small values $\omega \ll \omega_0$ [28, 30]. (See the discussion in Sect. 4.2.2 for more details.)

If this branching dynamics was to remain unmodified down to arbitrarily small values of ω , then the whole energy would end up into a ‘condensate’ at $\omega = 0$ [28]. In reality though, we expect the gluon cascade to terminate at the thermal scale T , because the very soft quanta with $\omega \lesssim T$ can efficiently thermalize via elastic collisions (see the discussion in the next subsection). If the medium acts as a *perfect sink* at the lower end of the cascade — in the sense of absorbing all the quanta with $\omega \lesssim T$ without modifying the dynamics of branching at higher energies $\omega \gg T$ — then the whole energy carried by the turbulent flow is eventually transmitted to the medium. Under this assumption, the total energy loss by the jet towards the medium is obtained as [28, 30]

$$\Delta E_{\text{flow}} \simeq \frac{v}{2} \omega_{\text{br}}(L) = \frac{v}{2} \bar{\alpha}^2 \hat{q} L^2, \quad (2.6)$$

with $v \simeq 4.96$. This result, which is independent of the initial energy E of the LP and grows with the medium size like L^2 , truly applies (under the ‘perfect sink’ assumption) for a very energetic jet with $E \gg \omega_{\text{br}}(L)$. In the opposite limit where $E \lesssim \omega_{\text{br}}(L)$ (the case of a mini-jet), one rather has $\Delta E_{\text{flow}} \simeq E$ (see Eq. (4.30) for a more general expression). Eq. (2.6) admits a natural physical interpretation [30]: the LP radiates an average number $v/2$ of primary gluons with energies of order $\omega_{\text{br}}(L)$, which then transmit their whole energy to the medium, via democratic branchings followed by the thermalization of the soft gluons ($\omega \sim T$) at the lower end of the cascades. We shall later discover that the assumption that the medium acts as a ‘perfect sink’ has some limitations in practice, yet it can be used for qualitative considerations and parametric estimates.

Another important assumption that was implicitly postulated by previous analyses of multiple branching [28, 30] is that the branching dynamics is *linear*, meaning that the gluons from the cascade can split, but not also recombine with each other. This assumption is correct provided the partons cascade are sufficiently dilute. The precise condition is that $f(t, \mathbf{x}, \mathbf{p}) \ll 1$, where $f(t, \mathbf{x}, \mathbf{p})$ is the *gluon phase-space occupation number* (below, N_g the total number of gluons in the jet),

$$f(t, \mathbf{x}, \mathbf{p}) \equiv \frac{(2\pi)^3}{2(N_c^2 - 1)} \frac{dN_g}{d^3\mathbf{x}d^3\mathbf{p}}. \quad (2.7)$$

³This upper limit ω_c on the energy of medium-induced gluon emissions follows from the condition that the gluon formation time $t_{\text{form}}(\omega)$ be at most as large as L .

This quantity has not been explicitly computed in the previous studies, but it is straightforward to obtain an order-of-magnitude estimate for it via physical considerations.

Consider a typical mini-jet, as generated by a primary gluon with initial energy $\omega_0 \lesssim \omega_{\text{br}}(L)$. Over a time interval of order $t_{\text{br}}(\omega_0)$, this whole energy gets redistributed, via multiple branching, among a large number $N_g \simeq \omega_0/T$ of soft quanta with energies $\omega \sim T$. Their occupancy can therefore be estimated as

$$f(T) \sim \frac{1}{N_c^2} \frac{\omega_0/T}{p_z \Delta z \Delta p_\perp^2 \Delta x_\perp^2}, \quad (2.8)$$

where $p_z \sim \omega \sim T$, Δp_\perp^2 is the transverse momentum squared acquired by a gluon via rescattering in the medium, Δz is the longitudinal extent of the distribution, and Δx_\perp^2 is the corresponding spread in the transverse plane.

The transverse phase-space $\Delta p_\perp^2 \Delta x_\perp^2$ occupied by a gluon with energy $\omega \sim p_z$ turns out to be independent of ω . Indeed, during a time Δt , a gluon accumulates a transverse momentum broadening $\Delta p_\perp^2 \simeq \hat{q} \Delta t$, leading to an uncertainty

$$\Delta x_\perp^2 \simeq \frac{\Delta p_\perp^2}{p_z^2} \Delta t^2 \simeq \frac{\hat{q} \Delta t^3}{\omega^2} \quad (2.9)$$

in its transverse location. Taking Δt of the order of the gluon lifetime, $\Delta t \sim t_{\text{br}}(\omega)$, one finds

$$\Delta p_\perp^2 \Delta x_\perp^2 \simeq \left(\frac{\hat{q} t_{\text{br}}^2(\omega)}{\omega} \right)^2 \sim \frac{1}{\bar{\alpha}^4}. \quad (2.10)$$

This is independent of ω , as anticipated, and parametrically large. Eq. (2.10) is truly a lower limit, since the soft gluons can also inherit part of the transverse momentum of their harder parents. The above argument also shows that, so long as $\omega \gg T$ — as is the case for the gluons which control the splitting process — the transverse momenta remain much smaller than the longitudinal ones: $p_\perp \ll p_z \simeq \omega$.

Consider now the longitudinal distribution of the soft quanta within the mini-jet. As already discussed, soft gluons are emitted promptly, so they can be produced anywhere along the cascade. After being emitted, they efficiently lose energy and randomize their direction of motion, via elastic collisions. Accordingly, they separate from each other and also from the harder ($p \gg T$) partons in the mini-jet over a time interval $\sim t_{\text{rel}}$, which is small compared to the overall lifetime $\sim t_{\text{br}}(\omega_0)$ of the cascade. Hence, on the average, these soft gluons should be quasi-uniformly distributed along z , within a distance $\Delta z \sim t_{\text{br}}(\omega_0)$. Using this, together with (2.8) and (2.10), we finally deduce

$$f(T) \sim \frac{\bar{\alpha}^4}{N_c^2} \frac{\omega_0}{T^2 t_{\text{br}}(\omega_0)}. \quad (2.11)$$

This number increases with ω_0 , so it is interesting to evaluate it for the largest possible value $\omega_0 \sim \omega_{\text{br}}(L)$ — the one which also controls the energy loss by the overall jet (cf. Eq. (2.6)). In that case, $t_{\text{br}}(\omega_0) \simeq L$, so one finds

$$f(T) \sim \frac{\bar{\alpha}^6}{N_c^2} \frac{\hat{q} L}{T^2}. \quad (2.12)$$

The corresponding estimate for the jet as a whole can be simply obtained by multiplying this result by a number $\sim \nu$, cf. Eq. (2.6). The occupation number (2.12) is parametrically small at weak coupling

and furthermore suppressed at large N_c . It is easy to check that the condition $f(T) \ll 1$ is always very well satisfied in practice.

The estimate in Eq. (2.12) should be more properly viewed as a *lower* limit on f : as we shall explain in Sect. 4.2.2, the soft gluons with $\omega \sim T$ are more abundantly produced during the late stages of the cascade, at times $t \sim t_{\text{br}}(\omega_0)$, so their distribution in z is not really homogeneous. (This will be also confirmed by the numerical simulations in Sect. 5; see in particular Fig. 8.) An *upper* limit on the longitudinal occupancy is however easily obtained by assuming the smallest possible longitudinal spread for the soft gluons, namely their lifetime $t_{\text{br}}(T)$. With $\Delta z \sim t_{\text{br}}(T)$ and $\omega_0 \sim \omega_{\text{br}}(L)$, Eq. (2.8) implies (recall that $t_{\text{br}}(T) \sim 1/\bar{\alpha}^2 T$),

$$f(T) \sim \frac{\bar{\alpha}^4}{N_c^2} \frac{\omega_{\text{br}}(L)}{T^2 t_{\text{br}}(T)} \sim \frac{\bar{\alpha}^8}{N_c^2} \frac{\hat{q} L^2}{T}, \quad (2.13)$$

which is still much smaller than one in all practical situations of interest, as one can easily check.

For what follows, one should keep in mind that the previous estimates for f refer exclusively to the soft gluons generated by the jet via multiple branching. When $\omega \sim T$, these gluons add to those from the background medium, whose occupation numbers are given by the usual, Bose-Einstein, thermal distribution and hence are of order one. So the present results also show that the effect of the jet on the occupancy of gluons with $\omega \lesssim T$ represents only a small perturbation. This in particular implies that the jet cannot produce ‘hot spots’ in the medium (it cannot significantly increase the local energy density): the energy density carried by the soft jet constituents with $\omega \sim T$ is obtained by multiplying $f(T)$ by $N_c^2 T^4$ and hence remains much smaller than the respective quantity for the thermal gluons, i.e. $\varepsilon \sim N_c^2 T^4$, so long as $f(T) \ll 1$.

2.2 Elastic collisions and thermalization

In the discussion in the previous subsection, we have implicitly assumed that the only effect of the elastic collisions between the gluons from the jet and the medium constituents is to trigger new branchings. In reality though, such interactions can also transfer energy and momentum between the colliding particles, leading to energy loss and momentum broadening for the jet constituents. As we shall see, these effects remain negligible so long as the gluons in the cascade have relatively large energies $\omega \gg T$, but they become a leading-order effect, and the driving force towards thermalization, when $\omega \sim T$.

To propose a theoretical description for these interactions, it is essential to recall, from the previous discussion, that the gluon system produced via multiple branching is dilute. Hence, it is appropriate to study the effects of elastic collisions on individual gluons from the jet. So long as the gluon under study has a relatively large energy $\omega \gg T$, it can be unambiguously distinguished from the thermal gluons, so it is possible to describe its dynamics by using the same methods as for other energetic probes, like a relativistic heavy quark (see e.g. [44–47]). In this subsection we shall use a Langevin description because of its formal simplicity. Later on, we shall employ the equivalent method of the Fokker-Planck equation for more elaborate studies. Strictly speaking, both descriptions will eventually fail when the energy of the ‘probe’ gluon decreases down to $\omega \sim T$, but even in that case they remain qualitatively correct, in that they capture the correct time scale for thermalization to parametric accuracy.

For more clarity, let us first assume that the branching dynamics is switched off, meaning that the energetic gluon suffers only elastic collisions in the plasma. The Langevin equation which encompasses

the effects of these collisions reads as follows:

$$\frac{dp^i}{dt} = -\eta v^i + \xi^i, \quad \langle \xi^i(t) \xi^j(t') \rangle = \frac{\hat{q}}{2} \delta^{ij} \delta(t - t'), \quad (2.14)$$

where $v^i = p^i/p$, with $i = 1, 2, 3$, is the particle velocity, η is a friction coefficient, and ξ^i is a stochastic force (the ‘noise’). Microscopically, the total force in the r.h.s. of Eq. (2.14) represents the Lorentz force generated by random, quasi-classical, fields in the plasma — the color fields of the thermal particles, which are slightly disturbed out-of-equilibrium by their scattering with the external particle. The ‘drag force’ $f^i = -\eta v^i$ describes the average effect of this microscopic force, which is the energy transfer from the probe to the medium, whereas the noise term ξ^i represents its random component leading to momentum broadening. The average over the noise reflects the thermal average over the microscopic sources of this force. The facts that the noise correlator is local in time (‘white noise’) and also isotropic are non-trivial and reflect some approximations. The first property is true because we follow the dynamics on time scales much larger than the typical correlation time for the sources. The isotropy is ‘accidental’ (at least in the relativistic context at hand), in the sense that it is specific to the lowest-order approximation at weak coupling and to the ultrarelativistic limit for the external particle⁴ [45].

By using a properly discretized version of the stochastic equation (2.14) (see e.g. [45]), one can deduce the following evolution equation for the average of the particle momentum squared:

$$\frac{d\langle p^2 \rangle}{dt} = -2\eta \langle p \rangle + \frac{3}{2} \hat{q}. \quad (2.15)$$

For this equation to be consistent with the approach towards the thermal distribution⁵ $f_p \propto e^{-p/T}$ (which in turn implies $\langle p \rangle = 3T$ and $\langle p^2 \rangle = 12T^2$), one needs to fulfill the Einstein relation $\hat{q} = 4T\eta$ between diffusion and drag. This is indeed guaranteed by the fluctuation-dissipation theorem for thermal correlations.

Let us now assume that the energetic gluon enters the medium at $t = 0$ with a large momentum $p_0 \gg T$ oriented along the z axis ($i = 3$): $v_z \equiv v^3 = 1$. At early stages, the longitudinal momentum remains large, $p_z \gg T$, and the effects of fluctuations are unimportant: $p_\perp \ll p_z$ and $v_z \simeq 1$. During these stages, one can take the average in Eq. (2.14) to deduce $d\langle p_z \rangle / dt \simeq -\eta$ and therefore $\langle p_z(t) \rangle \simeq p_0 - \eta t$. This shows that the particle loses most of its energy, from the initial value $p_0 \gg T$ down to a value $p \sim T$ where diffusion effects start to be important, over an interval $\Delta t \simeq p_0/\eta = (p_0/T)t_{\text{rel}}$, with

$$t_{\text{rel}} \equiv \frac{4T^2}{\hat{q}} \sim \frac{1}{\bar{\alpha}^2 T \ln(1/\bar{\alpha})}. \quad (2.16)$$

From that moment on, the particle approaches the thermal distribution quite fast, over a time $\Delta t \sim t_{\text{rel}}$, under the combined effect of drag and diffusion. This can be understood from the fact that its momentum broadening increases with time like $\langle p^2 \rangle \simeq (3/2)\hat{q}\Delta t$, cf. Eq. (2.15), and hence it becomes

⁴In general, $(\hat{q}/2)\delta^{ij}$ in the r.h.s. of the noise correlator gets replaced by $\hat{q}^{ij} = \hat{q}_\ell \hat{v}^i \hat{v}^j + (\hat{q}/2)(\delta^{ij} - \hat{v}^i \hat{v}^j)$, where the longitudinal (\hat{q}_ℓ) and transverse (\hat{q}) momentum diffusion coefficients are different from each other. But for a massless energetic particle and in the lowest, leading-logarithmic, approximation, it so happens that $\hat{q}_\ell = \hat{q}/2$; see e.g. [45, 47, 49].

⁵The probe gluon is here treated as a classical particle, hence its momentum distribution in thermal equilibrium is the relativistic version of the classical Maxwell-Boltzmann distribution, also known as the Maxwell-Jüttner distribution.

of $\mathcal{O}(T^2)$ after a time $\Delta t \sim T^2/\hat{q} \sim t_{\text{rel}}$. Clearly, when $p_0 \gg T$, the total duration of the thermalization process is controlled by the first period — the energy loss via drag — and is of order $t_{\text{th}}(p_0)$, with

$$t_{\text{th}}(p) \equiv \frac{p}{T} t_{\text{rel}} = \frac{4pT}{\hat{q}}. \quad (2.17)$$

Let us now switch on the branching dynamics, on top of the elastic collisions. From the previous subsection, we know that the incoming gluon with energy $p_0 \gg T$ has a lifetime $\Delta t \sim t_{\text{br}}(p_0)$ before it undergoes a first democratic branching. By comparing Eqs. (2.5) and (2.17), it is clear that $t_{\text{br}}(p_0) \ll t_{\text{th}}(p_0)$ so long as $p_0 \gg T$. Indeed,

$$\frac{t_{\text{br}}(p)}{t_{\text{th}}(p)} = \frac{1}{4\bar{\alpha}} \sqrt{\frac{\hat{q}}{pT^2}} \sim \sqrt{\frac{T}{p}}, \quad (2.18)$$

where we have used $\hat{q} \sim \bar{\alpha}^2 T^3$ for the weakly-coupled QGP. This implies that the incoming gluon disappears via branching before having the time to lose a substantial fraction of its original energy via drag. A similar conclusion applies to all the successive generations within the ensuing gluon cascade, so long as the respective momenta are hard, $p \gg T$: the elastic collisions cannot significantly modify the kinematics of the hard gluons during the time interval between two successive democratic branchings.

However, the situation changes in the later stages of the cascade when, as a result of successive branchings, the gluons have been degraded to lower energies $p \sim T$. Then, the various time-scales previously introduced become degenerate (at least, parametrically),

$$t_{\text{br}}(T) \sim t_{\text{th}}(T) \sim t_{\text{rel}} \sim \frac{1}{\bar{\alpha}^2 T \ln(1/\bar{\alpha})}, \quad (2.19)$$

meaning that the various processes start to compete with each other. Before they have the time to branch again, the gluons with $p \sim T$ can lose a substantial fraction of their energy towards the medium and also suffer a considerable broadening of their momentum distribution. Such (drag and diffusion) processes will naturally drive the soft gluons towards a thermal distribution in momentum which, within the present approximations, appears to be the classical, Maxwell-Boltzmann, distribution. In reality though, our approximations fail to properly describe the final equilibrium state, for the reasons already explained. The gluons from the jet which approach thermal equilibrium cannot be distinguished anymore from the gluons in the plasma, so a proper theoretical description of the late stages should rather follow the *complete* gluon distribution. For the latter, the effects of the quantum statistics are essential (since the occupation numbers are of order one) and the final distribution in equilibrium must be of the Bose-Einstein type. When this equilibrium distribution is finally reached, the branching process naturally stops, because of the compensation between splittings and recombination (see the discussion in Sect. 3 below). Thus the cascade effectively ends at a scale $\sim T$.

This discussion shows that the characteristic time scale for the thermalization of a mini-jet — the duration of the overall process which starts with the emission of a primary gluon with energy $p_0 \gg T$ and ends up with the thermalization of its soft branching products — is controlled by the branching part of the dynamics and hence is of order $t_{\text{br}}(p_0)$. As discussed around Eq. (2.18), this time scale $t_{\text{br}}(p_0)$ is much smaller than $t_{\text{th}}(p_0)$ — the would-be thermalization time for a gluon with the same initial energy in the absence of branchings. This is so since the branchings are more efficient than the elastic collisions in degrading the energy of the relatively hard ($p \gg T$) constituents of the jet.

In the previous considerations, we have focused on the relaxation of the *energy-momentum* distribution, but we ignored the *spatial* distribution of the gluons inside the jet. In particular, we have discarded the fact that this distribution is highly inhomogeneous to start with — the leading particle and, more generally, all the energetic constituents of the jet with $p \gg T$ propagate at the speed of light and are concentrated near the light-cone ($z = t$) —, a feature which could prevent, or at least delay, thermalization. Also, we have implicitly assumed that the dynamics responsible for thermalization at the low-energy end of the cascade ($p \sim T$) does not affect the branching dynamics at higher energies $p \gg T$. In order to address such complex issues, test our various assumptions, and thus firmly establish the physical picture that we previously exposed, we need more explicit calculations. A suitable formalism in that sense will be described in the next section.

3 The kinetic equation for the longitudinal dynamics

In what follows we shall propose a relatively simple kinetic equation which captures the general dynamics exposed in the previous section, in the sense that it respects the various parametric estimates and thus is expected to reproduce the correct physical picture, and which allows for explicit studies, via semi-analytic and numerical techniques.

The starting point is a kinetic equation introduced in Ref. [36] and thoroughly derived in Refs. [43] (see also Refs. [27, 29] for a careful analysis of the quantum branching process, which justifies treating the successive branchings as independent from each other), with the schematic structure

$$\left(\frac{\partial}{\partial t} + \mathbf{v} \cdot \nabla_{\mathbf{x}} \right) f(t, \mathbf{x}, \mathbf{p}) = \mathcal{C}_{\text{el}}[f] + \mathcal{C}_{\text{br}}[f]. \quad (3.1)$$

Here, f is the gluon occupation number defined in Eq. (2.7), which *a priori* refers to gluons from both the jet and the surrounding medium⁶, $\mathcal{C}_{\text{el}}[f]$ is a collision integral encoding the effects of $2 \rightarrow 2$ elastic collisions, whereas $\mathcal{C}_{\text{br}}[f]$ encodes the inelastic processes, like $2 \rightarrow 3$ collisions, which lead to (collinear) branchings. The most general structure of these collision terms can be found in [43, 50], while a simpler form of $\mathcal{C}_{\text{br}}[f]$, which is sufficient for our present purposes, is presented in [36]. These general collision terms are non-linear with respect to the gluon occupation number, in such a way to respect the detailed balance principle and the quantum statistics. Accordingly, the thermal Bose-Einstein distribution is a fixed point for both $\mathcal{C}_{\text{el}}[f]$ and $\mathcal{C}_{\text{br}}[f]$.

The general equation (3.1) is difficult to solve in practice, because of the non-linear effects alluded to above and also because of the generally complicated structure of the two collision integrals, which involve multi-dimensional momentum integrations together with complicated kernels (see [43, 47] for details). Numerical solutions have been presented for special limits of this equation [39, 51, 52], which however do not cover the present physical situation. Here, however, we shall follow a different strategy: motivated by the physical discussion in the previous sections, we shall propose a simplified version of the kinetic equation, which allows for efficient numerical studies and even for piecewise analytic solutions. Similar approximations have been already used in the literature, separately for the elastic collisions and for the branching dynamics, but here we shall combine them for the first time in a study of the jet thermalization.

⁶To Eq. (3.1), one should add corresponding equations for the quark and the antiquark occupation numbers, but here these are not necessary, since the (anti)quarks will only appear as constituents of the thermal medium.

First, we would like to write an equation for the gluons from the jet alone, with the surrounding medium treated as a thermal bath which influences the jet dynamics but is not significantly disturbed by the latter. The omission of the back-reaction is indeed well justified, given that the gluonic system produced via branching remains dilute ($f(p) \ll 1$) down to the thermal scale $p \sim T$, as we have seen. By the same token, the kinetic equation can be *linearized* w.r.t. the occupation number f for the gluons in the jet.

The distinction between the gluons in the jet and those in the medium is strictly possible for the energetic quanta with $p \gg T$, which control most stages of the branching process, but it becomes ambiguous at later stages, notably during the thermalization process, where all the gluons have $p \lesssim T$. Notwithstanding, the discussion in the previous sections shows that the dynamics is rather smoothly changing around $p \sim T$, where the relevant time scales become commensurable with each other, cf. Eq. (2.19). Hence, there should be no danger (to parametric accuracy, at least) with extrapolating down to $p \sim T$ an equation which is strictly valid for $p \gg T$. With that in mind, one can deduce rather simple approximations to the collision integrals in Eq. (3.1).

Consider the elastic collisions first, which preserve the number of particles. Due to the infrared singularity of the Coulomb exchanges, the dominant contribution to the elastic collision integral comes from the small angle scatterings, i.e. from collisions where the momentum transfer between the colliding particles — here, a gluon from the jet and another one from the thermal bath — is much smaller than the individual momenta of these particles. More precisely, this property holds to leading logarithmic accuracy, since the momentum exchanges within the range $m_D \ll q \ll T$ produce a Coulomb logarithm $\ln(T^2/m_D^2) \sim \ln(1/\alpha_s)$ in the relevant transport coefficient (see below). Within this approximation, $\mathcal{C}_{\text{el}}[f]$ can be replaced with the Fokker-Planck dynamics, i.e. the sum of diffusion and drag [44–47]

$$\mathcal{C}_{\text{el}}[f] \simeq \frac{1}{4} \hat{q} \nabla_{\mathbf{p}} \cdot \left[\left(\nabla_{\mathbf{p}} + \frac{\mathbf{v}}{T} \right) f \right]. \quad (3.2)$$

In writing this expression, we have exploited the isotropy of the diffusion tensor and the Einstein relation between drag and diffusion, as already discussed in relation with Eq. (2.14). In fact, there is a one-to-one correspondence between the Langevin dynamics described by Eq. (2.14) and the Fokker-Planck dynamics encoded in the r.h.s. of Eq. (3.2). In particular, it is easy to check that the above collision term admits the classical thermal distribution (the Maxwell-Boltzmann distribution for a massless particle) as a fixed point: $\mathcal{C}_{\text{el}}[f_{\text{eq}}] = 0$ for $f_{\text{eq}}(\mathbf{p}) = \kappa e^{-p/T}$, where κ is independent of \mathbf{p} , but otherwise arbitrary. Clearly, one cannot expect gluons to obey a classical distribution in thermal equilibrium, yet one can rely on this Fokker-Planck dynamics to qualitatively study the *approach* towards equilibrium for the gluons from the jet, which have low occupancy. The relevant mechanism at work (elastic collisions with the thermal particles) and the characteristic time scales (namely $t_{\text{th}}(p)$ for energy loss, cf. Eq. (2.17), and t_{rel} for momentum broadening, cf. Eq. (2.16)) are correctly captured by Eq. (3.2), to parametric accuracy at least.

For a dilute quark-gluon plasma (QGP) and to the leading logarithmic accuracy of interest, \hat{q} is given by [45, 47, 49, 53]

$$\begin{aligned} \hat{q} &= 8\pi\alpha_s^2 N_c \ln \left(\frac{\langle k_{\text{max}}^2 \rangle}{m_D^2} \right) \int \frac{d^3\mathbf{p}}{(2\pi)^3} [N_c f_{\text{BE}}(1 + f_{\text{BE}}) + N_f f_{\text{FD}}(1 - f_{\text{FD}})] \\ &= \alpha_s N_c T m_D^2 \ln \left(\frac{\langle k_{\text{max}}^2 \rangle}{m_D^2} \right), \end{aligned} \quad (3.3)$$

where m_D is the leading-order result for the Debye screening mass, that is,

$$m_D^2 = \frac{2\pi}{3} \alpha_s T^2 (2N_c + N_f), \quad (3.4)$$

N_f is the number of active quark flavors, $\langle k_{\max}^2 \rangle \sim T^2$ is the maximal momentum transfer squared between the probe gluon and the medium constituents, and we have included contributions from both thermal gluons and thermal quarks, with respective occupation numbers

$$f_{\text{BE}}(p) = \frac{1}{e^{\frac{p}{T}} - 1}, \quad f_{\text{FD}}(p) = \frac{1}{e^{\frac{p}{T}} + 1}. \quad (3.5)$$

For the inelastic collision integral $\mathcal{C}_{\text{br}}[f]$, one can use the corresponding approximation in Ref. [36], which describes medium-induced gluon branching in the LPM regime, with the BDMPSZ branching rate shown in Eq. (2.1). The original equation in [36] involves both splitting ($1 \rightarrow 2$) and recombination ($2 \rightarrow 1$) processes, but only the splitting terms survive after linearizing w.r.t. the gluon occupation number. The ensuing expression reads (see also Refs. [27, 29])

$$\mathcal{C}_{\text{br}}[f] \simeq \frac{1}{t_{\text{br}}(p)} \int_0^1 dx \mathcal{K}(x) \left[\frac{1}{x^{\frac{5}{2}}} f\left(t, \mathbf{x}, \frac{\mathbf{p}}{x}\right) - \frac{1}{2} f(t, \mathbf{x}, \mathbf{p}) \right] \quad (3.6)$$

with $t_{\text{br}}(p)$ as defined in Eq. (2.5) and⁷

$$\mathcal{K}(x) \equiv \frac{[1 - x(1 - x)]^{\frac{5}{2}}}{[x(1 - x)]^{\frac{3}{2}}}. \quad (3.7)$$

We recall that x and $1 - x$ represent the longitudinal momentum fractions of the daughter gluons. The two terms in the r.h.s. of Eq. (3.6) are recognized as the gain and loss terms associated with a collinear splitting: in the gain term, a gluon with 3-momentum \mathbf{p} is produced via the splitting of a parent gluon with momentum \mathbf{p}/x ; in the loss term, a gluon with momentum \mathbf{p} disappears because it splits. The integrand has singularities at $x = 0$ and $x = 1$, which however cancel between the gain and loss terms, and the integral is well defined. One can easily check that the branching integral (3.7) preserves the total energy: $\int d^3\mathbf{p} |\mathbf{p}| \mathcal{C}_{\text{br}}[f](\mathbf{p}) = 0$.

Notice that the r.h.s. of Eq. (3.6) does not vanish when f approaches the thermal distribution $f_{\text{eq}}(\mathbf{p}) \propto e^{-p/T}$. (The only fixed point of this particular collision integral is the turbulent spectrum $f \propto 1/p^{7/2}$ [28, 36, 48].) However, from the previous discussion, we also know that the branching term in Eq. (3.6) is strictly correct only when $p \gg T$. On one hand, the mechanism which triggers radiation changes around $p \sim T$, from multiple scattering to single scattering, so the correct branching rate at lower momenta should be of the Bethe-Heitler type. On the other hand, the gluons from the jet having $p \lesssim T$ cannot be distinguished from the thermal gluons; so, in this soft region of the phase-space, the collision integrals should involve the *total* occupation number (medium plus jet), including the associated non-linear effects. This total occupation number efficiently relaxes to the Bose-Einstein distribution. When this happens, the non-linear terms — which are omitted in Eq. (3.6), but would be

⁷Strictly speaking, the jet quenching parameter \hat{q} which enters the expression (2.5) for the branching time is not exactly the same as that occurring in the Fokker-Planck term, Eq. (3.2), because of the difference between the respective transverse scales $\langle k_{\max}^2 \rangle$: one has $\langle k_{\max}^2 \rangle \sim T^2$ for the Fokker-Planck dynamics and, roughly, $\langle k_{\max}^2 \rangle \sim \hat{q} t_{\text{br}} \gg T^2$ for the branching of sufficiently energetic gluons (see the discussion in [54, 55]). Here however we shall ignore this subtle difference, which is anyway small, due to the weak, logarithmic, dependence upon $\langle k_{\max}^2 \rangle$, cf. Eq. (3.3).

present in a more general version of \mathcal{C}_{br} valid at soft momenta [36, 43] — will also stop the branching process.

However, this physical mechanism for stopping the branchings is not included in our linear equation, which applies to the gluon distribution created by the jet *alone*. To cope with that while keeping the formalism as simple as possible, we shall cut off by hand the branching process at some arbitrary scale $p_* \sim T$. In practice, we shall enforce the condition $p \geq p_*$ for all the particles participating in a $1 \rightarrow 2$ splitting process, that is, we shall require $p \geq p_*$ for the daughter gluons and hence $p \geq 2p_*$ for their parent. This cutoff p_* should be viewed as a free parameter of our model: the dependence of our predictions upon this scale, which as we shall see is weak so long as p_* remains of $\mathcal{O}(T)$, is indicative of the error that we have introduced by neglecting the non-linear terms in the (total) occupation number.

To summarize, our basic kinetic equation reads (with the compact notation $f_{\mathbf{p}} \equiv f(t, \mathbf{x}, \mathbf{p})$)

$$\left(\frac{\partial}{\partial t} + \mathbf{v} \cdot \nabla_{\mathbf{x}}\right) f_{\mathbf{p}} = \frac{1}{4} \hat{q} \nabla_{\mathbf{p}} \cdot \left[\left(\nabla_{\mathbf{p}} + \frac{\mathbf{v}}{T} \right) f_{\mathbf{p}} \right] + \frac{1}{t_{\text{br}}(p)} \int_r dx \mathcal{K}(x) \left[\frac{1}{x^{\frac{5}{2}}} f_{\mathbf{p}} - \frac{1}{2} f_{\mathbf{p}} \right], \quad (3.8)$$

where the symbol \int_r denotes the restricted integration over x (see Sect. 5 for details). This equation should be solved with the following initial condition at $t = 0$:

$$f(t = 0, \mathbf{x}, \mathbf{p}) = \frac{(2\pi)^3}{2(N_c^2 - 1)} \delta^{(3)}(\mathbf{x}) \delta(p_z - E) \delta^{(2)}(\mathbf{p}_{\perp}), \quad (3.9)$$

which represents the leading particle propagating along the z axis with energy $E \gg T$.

Eq. (3.8) matches our present purposes: it correctly encodes the dynamics of the relatively hard constituents of the jet with $p \gg T$ and, when extrapolated down to $p \lesssim T$, it also describes (at least to parametric accuracy) their approach to *kinetic* equilibrium — that is, the fact that the gluons from the jet individually approach a Maxwell-Boltzmann distribution in momentum, via elastic collisions in the plasma. On the other hand, the approach to *chemical* equilibrium — the evolution of the ensemble of the complete gluon distribution (jet+medium) towards the quantum Bose-Einstein distribution — is not encoded in this equation, but merely mimicked in a rather crude way by the lower cutoff p_* on the branching process.

Albeit considerably simpler than the original equations, Eq. (3.8) is still too complicated to be solved as it stands, including via numerical techniques. A main source of complication is the spatial inhomogeneity inherent in our problem, which is very strong to start with, cf. Eq. (3.9), and plays an essential role in the subsequent dynamics. In order to keep the salient features of this evolution in a numerically tractable way, we shall project Eq. (3.8) along the longitudinal axis and at the same time perform approximations based on the separation of scales $p_z \gg p_{\perp}$ between longitudinal and transverse momenta. This separation is physically realized so long as $p \gg T$, which is the regime where Eq. (3.8) strictly applies, but is progressively washed out when decreasing the momenta towards T . Yet, this approximation correctly keeps trace (to parametric accuracy, once again) of the separation of time scales in the problem: indeed, as already explained, the characteristic time scales for branching, Eq. (2.5), and for the thermalization of hard particles, Eq. (2.17), are controlled by the longitudinal momenta and become degenerate with each other (and with t_{rel} , Eq. (2.16)) only when $p \sim T$.

Specifically, by integrating Eq. (3.8) over the transverse phase-space, while at the same time approximating $p \simeq p_z$ within the definition of v_z , within $t_{\text{br}}(p)$, and within the condition $p \geq p_*$, we

finally obtain

$$\begin{aligned} \left(\frac{\partial}{\partial t} + v_z \frac{\partial}{\partial z}\right) f_\ell(t, z, p_z) &= \frac{1}{4} \hat{q} \frac{\partial}{\partial p_z} \left[\left(\frac{\partial}{\partial p_z} + \frac{v_z}{T}\right) f_\ell(t, z, p_z) \right] \\ &+ \frac{1}{t_{\text{br}}(p_z)} \int_r dx \mathcal{K}(x) \left[\frac{1}{\sqrt{x}} f_\ell\left(t, z, \frac{p_z}{x}\right) - \frac{1}{2} f_\ell(t, z, p_z) \right], \end{aligned} \quad (3.10)$$

where $v_z \equiv p_z/|p_z|$ and $f_\ell(t, z, p_z)$ is the longitudinal gluon distribution⁸,

$$f_\ell(t, z, p_z) \equiv \frac{dN_g}{dz dp_z} = \frac{2(N_c^2 - 1)}{(2\pi)^3} \int d^2 \mathbf{x}_\perp d^2 \mathbf{p}_\perp f(t, \mathbf{x}, \mathbf{p}). \quad (3.11)$$

In Eq. (3.10) it is understood that the partial derivative $\partial_{p_z} \equiv \partial/\partial p_z$ commutes with v_z : $\partial_{p_z}(v_z f_\ell) = v_z \partial_{p_z} f_\ell$. (This prescription follows for the limit $p_\perp \ll p_z$: starting with $v_z = p_z/p$ with $p = \sqrt{p_z^2 + p_\perp^2}$, one obtains $\partial_{p_z} v_z = p_\perp^2/p^3 \simeq p_\perp^2/p_z^3$, which is much smaller than the respective natural value $\sim 1/p_z$.)

Eq. (3.10) is the equation that we shall explicitly study in what follows, via a combination of analytic and numerical methods. To that aim, it is also useful to remind that the branching integral above admits the turbulent fixed point $f_\ell \propto 1/p_z^{3/2}$, which is expected to control the shape of the spectrum at intermediate momenta $p_* \ll p_z \ll E$.

4 Semi-analytic studies of the kinetic equation

As explained in the previous section, the two ‘collision terms’ in the r.h.s. of Eq. (3.10) become important in different kinematical regions, which are complementary to each other: the high-energy region at $p \gg T$ for the branching term and, respectively, the low-energy region at $p \lesssim T$ for the elastic collisions. This distinction makes it possible to *separately* study their physical consequences — at least, at a qualitative level. Namely, one can effectively treat the branching process as a *source* of relatively soft gluons, which get injected into the medium at a scale $p_* \sim T$ and subsequently feel the effects of elastic collisions, in the form of drag and diffusion. These considerations motivate the following, simplified, version of the kinetic equation (3.10) :

$$\left(\frac{\partial}{\partial t} + v \frac{\partial}{\partial z}\right) f(t, z, p) = \frac{1}{4} \hat{q} \frac{\partial}{\partial p} \left[\left(\frac{\partial}{\partial p} + \frac{v}{T}\right) f(t, z, p) \right] + \mathcal{S}(t, z, p; p_*). \quad (4.1)$$

(From now on, we shall omit the subscript ℓ on f as well as the subscript z on longitudinal momenta and velocities, to simplify notations.) Notice that, when using this source approximation, we implicitly assume that the medium acts as a perfect sink: the branching dynamics at $p > p_*$ is not at all affected by collisions. For consistency, one must also construct the source $\mathcal{S}(t, z, p)$ by assuming an ‘ideal’ gluon cascade, with wave turbulence, at $p > p_*$. This source has the general structure

$$\mathcal{S}(t, z, p; p_*) = \delta(t - z) \delta(p - p_*) \Gamma(t, p_*), \quad (4.2)$$

where $\Gamma(t, p_*)$ is the flux of gluons at the lower end of the cascade at time t . This flux can be easily inferred from the previous studies of the ‘ideal’ branching process [28, 30] and will be presented in Sect. 4.2.2 below. Our ultimate purpose in this section is to solve Eq. (4.1) with this particular source.

⁸Notice that this quantity f_ℓ is not an occupation number by itself (because of the integration over the transverse phase-space in Eq. (3.11)), so in practice one can very well have $f_\ell > 1$ and still use a linear kinetic equation, provided one can justify that the actual occupation number is indeed small.

In preparation to that, it will be useful to study a couple of simpler cases, which have a physical interest by themselves and for which we will be able to obtain exact solutions in analytic form. We shall start by considering in Sect. 4.1 a steady source which propagates at the speed of light. Then, in Sect. 4.2.1, we shall construct the exact Green’s function for the differential operator appearing in Eq. (4.1) (i.e. for the ultrarelativistic Fokker–Planck equation in 1+1 dimensions). Finally, in Sect. 4.2.2, we shall use this Green’s function to give a semi-analytic calculation of the gluon distribution produced by the physical source.

4.1 Thermalization for a steady source

In this subsection we shall present an exact solution for the case where the time-dependence of the injection rate $\Gamma(t, p_*)$ in the r.h.s. of Eq. (4.2) can be neglected. This is a good approximation if one is interested in the effects of the collisions over a time interval Δt which is much smaller than the characteristic time scale $t_{\text{br}}(E)$ for the evolution of the source via branchings, but much larger than t_{rel} (in order for the effects of collisions to be indeed significant); that is, $t_{\text{rel}} < \Delta t \ll t_{\text{br}}(E)$. During this time Δt , the source can be effectively treated as ‘frozen’ and the corresponding distribution at $z \leq t$ is expected to depend only on $t - z$.

For convenience, we choose to normalize the injection rate as $\Gamma(t, p_*) = T$. (This brings no loss of generality since the equation is linear.) Also, within the context of this subsection, it is preferable to denote the energy of the soft gluons as p_0 , rather than p_* . With these conventions, Eq. (4.1) becomes (below, a prime denotes a derivative w.r.t. \hat{p})

$$\left(\frac{\partial}{\partial \hat{t}} + v \frac{\partial}{\partial \hat{z}} \right) f = (f' + v f)' + \delta(\hat{t} - \hat{z}) \delta(\hat{p} - \hat{p}_0), \quad (4.3)$$

in terms of dimensionless variables which measure the respective quantities in natural units, that is, in units of t_{rel} for all the time and length scales ($\hat{t} = t/t_{\text{rel}}$, $\hat{z} = z/t_{\text{rel}}$) and in units of T for the various momenta ($\hat{p} = p/T$, etc). In what follows, we shall use such reduced variables in most formulæ, to simplify the notation, but we shall restore the physical units when discussing the physical interpretation of the results. Also, we shall drop the hat on the reduced variables (e.g. $\hat{p} \rightarrow p$), as the distinction should be clear from the context.

We search for a stationary distribution $f(x^-, p; p_0)$ with $x^- \equiv t - z$. This function obeys

$$\begin{cases} 0 = (f' + f)' + \delta(x^-) \delta(p - p_0) & \text{for } p > 0, \\ 2 \frac{\partial}{\partial x^-} f = (f' - f)' & \text{for } p < 0. \end{cases} \quad (4.4)$$

together with the condition for particle number conservation at $p = 0$:

$$(f' + f)|_{p=0^+} = (f' - f)|_{p=0^-} = \delta(x^-). \quad (4.5)$$

For $p > 0$ the solution to Eq. (4.4) is found in the form

$$f(x^-, p; p_0) = f_{\text{J}}(p, p_0) \delta(x^-) + C^+(x^-) e^{-p} \quad (4.6)$$

where $f_{\text{J}}(p, p_0)$ is the ‘jet front function’ (see also Fig. 2)

$$f_{\text{J}}(p, p_0) \equiv e^{-p} (e^{p_0} - 1) \theta(p - p_0) + (1 - e^{-p}) \theta(p_0 - p), \quad (4.7)$$

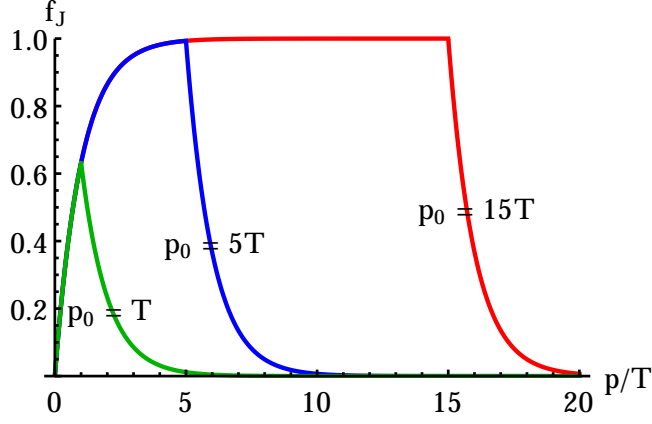


Figure 2. The jet front function $f_J(p, p_0)$ is displayed as a function of p for $p_0/T = 1, 5$ and 15 .

and $C^+(x^-)$ is an unknown function, to be later determined. For $p < 0$, it is convenient to use the Laplace transform of the solution, $f_s(p) \equiv \int_0^\infty dx^- e^{-sx^-} f(x^-, p; p_0)$. By taking the Laplace transform in the second equation (4.4), one obtains

$$f_s(p) = \tilde{C}^-(s) e^{\frac{p}{2}(\sqrt{1+8s}+1)} \quad \text{for } p < 0. \quad (4.8)$$

By imposing the conservation condition (4.5) (which actually introduce two constraints), we can determine both ‘coefficient’ functions $\tilde{C}^-(s)$ and $\tilde{C}^+(s)$ (the Laplace transform of $C^+(x^-)$):

$$\tilde{C}^+(s) = \tilde{C}^-(s) = \frac{2}{\sqrt{8s+1}-1} \quad (4.9)$$

After also performing the inverse Laplace transformation, we finally obtain

$$f(t-z, p; p_0) = \begin{cases} f_J(p, p_0) \delta(t-z) + \left[\frac{1}{4} \operatorname{erf} \left(\frac{\sqrt{t-z}}{2\sqrt{2}} \right) + \frac{1}{4} + \frac{e^{-\frac{t-z}{8}}}{\sqrt{2\pi}\sqrt{t-z}} \right] e^{-p} & \text{for } p \geq 0, \\ \frac{1}{4} e^p \left[\operatorname{erf} \left(\frac{2p+t-z}{2\sqrt{2}\sqrt{t-z}} \right) + 1 \right] + \frac{e^{-\frac{(-2p+t-z)^2}{8(t-z)}}}{\sqrt{2\pi}\sqrt{t-z}} & \text{for } p \leq 0. \end{cases} \quad (4.10)$$

We have introduced here the error function

$$\operatorname{erf}(x) \equiv \frac{2}{\sqrt{\pi}} \int_0^x dt e^{-t^2}. \quad (4.11)$$

By inspection of the solution in Eq. (4.10), one can recognize a *front* which propagates at the speed of light with the profile in p shown in Fig. 2, and a *tail* at $z < t$ which is localized around $p = 0$. The overall distribution is illustrated in Fig. 3 for the case $p_0 = T$, which is the most interesting one for the physical problem at hand (recall that $p_0 \equiv p_*$ is the infrared end of the gluon cascade). However, in order to better appreciate the physical content of this stationary distribution, it is useful to consider first the high-energy case $p_0 \gg T$. Then, as visible in Fig. 2, the front profile becomes a θ -function with support at $0 < p < p_0$. This can be understood as follows: a particle injected by the source at time t_0 with $p_0 \gg T$ loses energy towards the medium at a constant rate, via drag (recall the discussion following Eq. (2.14)); hence, its energy decreases with time according to

$$p(t) = p_0 - (T/t_{\text{rel}})(t - t_0). \quad (4.12)$$

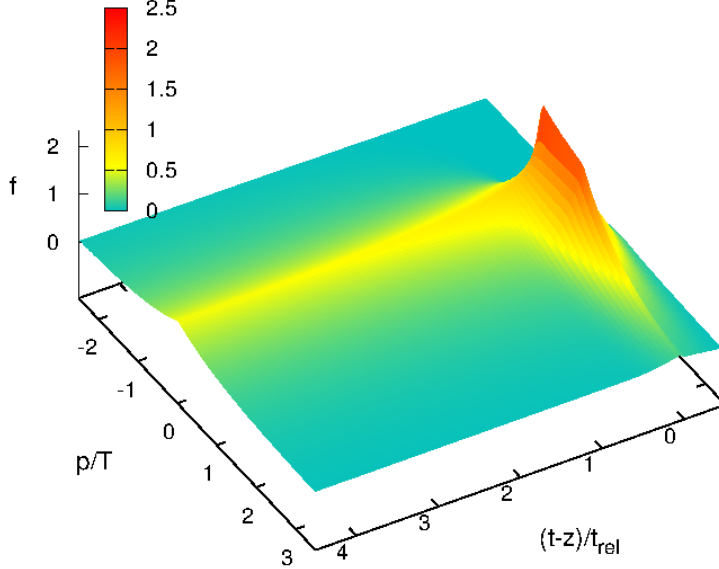


Figure 3. The distribution (4.10) as produced by a steady source is shown as a function of $t - z$ and p for $p_0 = T$. This figure exhibits a front moving along the light-cone at $z = t$ and a thermalized tail at $z \lesssim t - t_{\text{rel}}$. In displaying the front, the δ -function in Eq. (4.10) is regulated as $\delta_\epsilon(t - z) = \frac{1}{\sqrt{\epsilon\pi}} e^{-\frac{(t-z)^2}{\epsilon}}$ with $\epsilon = 0.1$.

So long as this energy remains much larger than T , which is indeed the case during a large interval $t - t_0 \simeq (p_0/T)t_{\text{rel}} \gg t_{\text{rel}}$, the diffusion effects are negligible and the distribution created by this particle can be as well studied by neglecting the second-order derivative f'' in Eq. (4.3). The corresponding solution is easily found as

$$f(t - z, p; p_0) = \delta(t - z)\theta(p_0 - p)\theta(p) \quad (\text{without diffusion}), \quad (4.13)$$

which is indeed very similar to the ‘front’ piece of Eq. (4.10) in the case $p_0 \gg T$. Hence, the ‘front’ is built with those particles that have been recently injected by the source, within a time interval $\Delta t = (p_0/T)t_{\text{rel}}$ prior to the time t of measurement, and which have a still a relatively large energy $p \gtrsim T$ at time t . All the other particles, that have been injected at earlier times $t' < t - (p_0/T)t_{\text{rel}}$, have been degraded by the viscous drag to energies $p \lesssim T$, where the diffusion effects *are* important. This becomes clear by inspection of the function $f_J(p, p_0)$ for $p_0 = 1$ in Fig. 2.

As a consequence of the competition between diffusion and drag, the gluons with $|p| \lesssim T$ can have both positive and negative velocities, hence their distribution moves at a slower speed $|v| < 1$. This explains the depletion visible in f_J at $p \lesssim T$ (for any p_0) and also the formation of the tail. At points sufficiently far away from the front, such that $t - z \gg t_{\text{rel}}$, the distribution reaches thermal equilibrium, since this is the fixed point of the Fokker-Plank dynamics. Indeed, the solution in Eq. (4.10) implies

$$f(t - z, p; p_0) \simeq \frac{1}{2} e^{-|p|/T} \quad \text{when } t - z \gg t_{\text{rel}}. \quad (4.14)$$

To understand the energy balance between the jet and the medium, notice that the external source in Eq. (4.3) inserts energy at a rate $dE_s/dt = p_0 T$, whereas the energy carried by the thermalized tail

$t - z \gg t_{\text{rel}}$ increases at a rate $dE_{\text{ther}}/dt = T^2$. (The total energy in the front is independent of time, $E_J = \int dp p f_J(p, p_0) \sim t_{\text{rel}} p_0^2$, and represents only a negligible fraction of the total energy injected by the source over large times.) If $p_0 \gg T$, then the insertion rate is much larger than the thermalization rate, meaning most of the energy is lost via viscous drag — meaning it is transferred via collisions to the medium constituents. By choosing $p_0 \simeq T$, i.e. by inserting the particles directly at the medium scale, we can minimize the effects of the drag and thus recover most of the injected energy in the thermalized tail.

The qualitative features that we have discovered in this simple example are in fact generic and will be recovered in the more general situations to be studied later on. In particular, the peculiar structure of the distribution visible in Fig. 3, with a jet localized on the light-cone ($z = t$) and a thermalized tail well behind it ($z < t - t_{\text{rel}}$), will also show up for a physical jet initiated by a leading particle with energy $E \gg T$, at least for sufficiently small times $t \lesssim t_{\text{br}}(E)$.

4.2 Jet quenching in the source approximation

In this subsection we shall use the source approximation, cf. Eq. (4.1), in order to unveil generic features of the jet evolution in the presence of both branchings and elastic collisions. The solution to Eq. (4.1) corresponding to a general source $\mathcal{S}(t, z, p)$ can be written as

$$f(t, z, p) = \int dp_0 dz_0 f_G(t, z - z_0, p, p_0) f_0(z_0, p_0) + \int dp_0 dz_0 \int_{-\infty}^t dt' f_G(t - t', z - z_0, p; p_0) \mathcal{S}(t', z_0, p_0), \quad (4.15)$$

where we have chosen the initial condition $f(0, z, p) = f_0(z, p)$ and f_G is the appropriate Green's function, that is, the solution to the homogeneous equation

$$\left(\frac{\partial}{\partial t} + v \frac{\partial}{\partial z} \right) f_G(t, z, p) = \frac{\partial}{\partial p} \left[\left(\frac{\partial}{\partial p} + v \right) f_G(t, z, p) \right], \quad (4.16)$$

with initial condition $f_G(0, z, p; p_0) = \delta(z) \delta(p - p_0)$ with $p_0 > 0$. An analytic form for this Green's function will be constructed in the next subsection and then applied to the source representing an ideal branching process, in Sect. 4.2.2.

4.2.1 The Fokker-Planck Green's function

The Green's function for the longitudinal Fokker-Planck equation can be constructed via a mathematical method similar to that described in the previous subsection for the case of a steady source. In what follows, we shall omit the details but merely show the starting point equations, which replace the previous equations (4.4) and (4.5). After performing Laplace and Fourier transforms with respect to t and z respectively, we deduce

$$\begin{cases} (s + iQ) - \delta(p - p_0) = f''_{sQ} + f'_{sQ} & \text{for } p > 0, \\ s f_{sQ} - iQ f_{sQ} = f''_{sQ} - f'_{sQ} & \text{for } p < 0. \end{cases} \quad (4.17)$$

together with the following condition for the number conservation

$$(f'_{sQ} + f_{sQ})|_{p=0^+} = (f'_{sQ} - f_{sQ})|_{p=0^-}, \quad (4.18)$$

where f_{sQ} is a compact notation for a function of two arguments, s and Q , defined as

$$f_{sQ} \equiv \int_0^\infty dt e^{-st} \int dz e^{-iQz} f(t, z, p). \quad (4.19)$$

After lengthy but straightforward mathematical manipulations, one finally obtains

$$f_G(t, z, p; p_0) = \theta(p) f_G^+(t, z, p; p_0) + \theta(-p) f_G^-(t, z, p; p_0), \quad (4.20)$$

where (with $t \geq |z|$)

$$\begin{aligned} f_G^+(t, z, p; p_0) &= \frac{e^{-\frac{p_0-p}{2}-\frac{t}{4}}}{2\sqrt{\pi t}} \left[e^{-\frac{(p-p_0)^2}{4t}} - e^{-\frac{(p+p_0)^2}{4t}} \right] \delta(t-z) \\ &+ \frac{e^{-\frac{(p+p_0-z)^2}{4t}-p}}{8\sqrt{\pi}t^{5/2}} [t(t+2) - (p+p_0-z)^2] \operatorname{erfc} \left(\frac{1}{2} \sqrt{t - \frac{z^2}{t}} \left(\frac{p+p_0}{t+z} - 1 \right) \right) \\ &+ \frac{(t+z)(p+p_0+t-z)}{4\pi t^2 \sqrt{t^2 - z^2}} e^{-\frac{(p+p_0)^2}{2(t+z)} + \frac{p_0-p}{2} - \frac{t}{4}}, \end{aligned} \quad (4.21)$$

and

$$\begin{aligned} f_G^-(t, z, p; p_0) &= \frac{(t+z)(p_0+t-z) - p(t-z)}{4\pi t^2 \sqrt{t^2 - z^2}} e^{-\frac{p^2}{2(t-z)} + \frac{p+p_0}{2} - \frac{p_0^2}{2(t+z)} - \frac{t}{4}} \\ &+ \frac{e^{p-\frac{(p+p_0-z)^2}{4t}}}{8\sqrt{\pi}t^{5/2}} [t(t+2) - (p+p_0-z)^2] \operatorname{erfc} \left(\frac{1}{2} \sqrt{t - \frac{z^2}{t}} \left(\frac{p_0}{t+z} - \frac{p}{t-z} - 1 \right) \right). \end{aligned} \quad (4.22)$$

In these formulæ, we have introduced the complementary error function $\operatorname{erfc}(x) \equiv 1 - \operatorname{erf}(x)$ (cf. Eq. (4.11)). Also, we have used reduced variables $p \rightarrow p/T$, $t \rightarrow t/t_{\text{rel}}$ etc., to simplify writing (recall the discussion after Eq. (4.3)). The above expression for f_G is normalized to unity w.r.t. these reduced variables: $\int dz dp f_G(t, z, p; p_0) = 1$. In order to obtain the properly normalized Green's function in physical units, one must divide the result in Eqs. (4.21)–(4.22) by the dimensionless product Tt_{rel} and replace all the reduced variables by their physical counterparts ($p \rightarrow p/T$, etc).

The above expression for f_G looks quite involved. In order to unveil its physical content, it is useful to first consider its simpler version obtained after integrating over z :

$$f_G(t, p; p_0) = \begin{cases} \frac{1}{4} e^{-p} \operatorname{erfc} \left(\frac{p+p_0-t}{2\sqrt{t}} \right) + \frac{1}{2\sqrt{\pi t}} e^{-\frac{(p-p_0+t)^2}{4t}} & \text{for } p > 0 \\ \frac{1}{4} e^p \operatorname{erfc} \left(\frac{-p+p_0-t}{2\sqrt{t}} \right) + \frac{e^p}{2\sqrt{\pi t}} e^{-\frac{(-p+p_0-t)^2}{4t}} & \text{for } p < 0. \end{cases} \quad (4.23)$$

This function describes the relaxation of an initial perturbation which is homogeneous in z but localized in momentum: $f_G(0, p; p_0) = \delta(p - p_0)$. For $p_0 \gg T$ and sufficiently small times, such that $\frac{t}{t_{\text{rel}}} \ll \frac{p_0}{T}$, $f_G(t, p; p_0)$ is dominated by its Gaussian component at $p > 0$, that is,

$$f_G(t, p; p_0) \simeq \frac{1}{2\sqrt{\pi t}} e^{-\frac{(p-p_0+t)^2}{4t}} \quad \text{when } t \ll p_0. \quad (4.24)$$

This describes the damping of the original energy via drag and also the broadening of the longitudinal momentum distribution due to diffusion, in agreement with the discussion in Sect. 2.2:

$$\langle p(t) \rangle \simeq p_0 - (T/t_{\text{rel}})t, \quad \langle p^2 \rangle - \langle p \rangle^2 \simeq 2\hat{q}t. \quad (4.25)$$

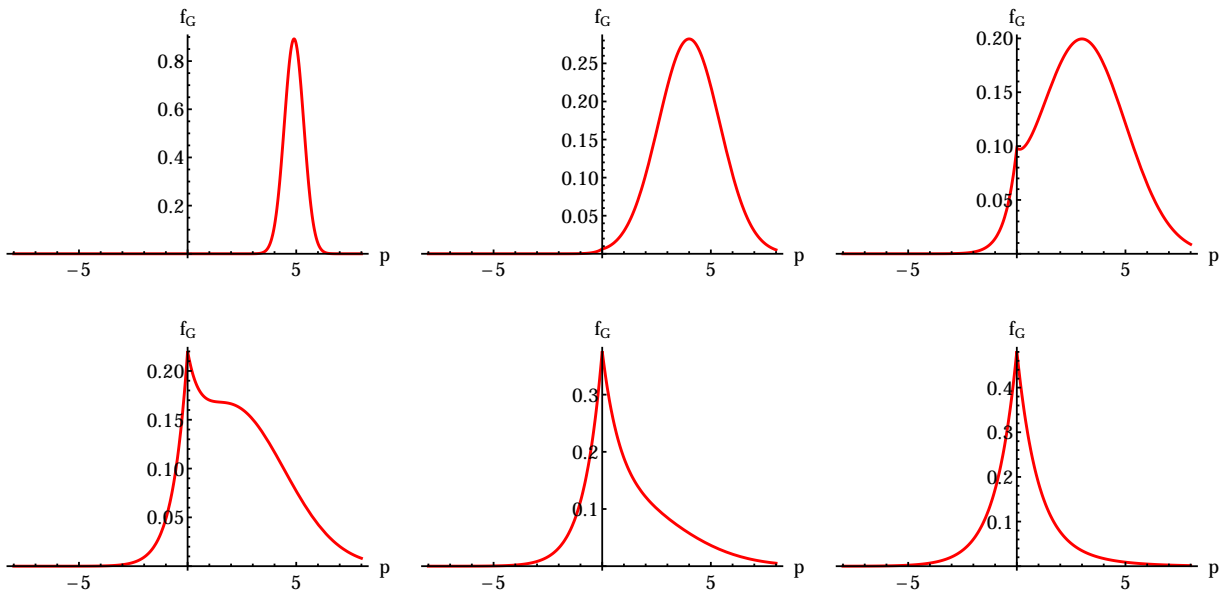


Figure 4. The ‘reduced’ Green’s function in Eq. (4.23) plotted as a function of p for $p_0 = 5$ and 6 successive values of time: $t = 0.1, 1, 2, 3, 5, 10$.

But already for such small values of time, there is a second component (represented by the two terms proportional to the complementary error function) which starts growing around $p = 0$. This corresponds to particles which have essentially lost their original energy and pile up around $p = 0$, via diffusion. For larger times $t \gtrsim (p_0/T)t_{\text{rel}}$, this component becomes the dominant one and rapidly approaches the thermal distribution (notice that $\text{erfc}(x) \rightarrow 2$ when $x \rightarrow -\infty$):

$$f_G(t, p; p_0) \simeq \frac{1}{2} e^{-|p|} \quad \text{when } t \gg p_0. \quad (4.26)$$

Turning now to the general case with z -dependence, Eqs. (4.21)–(4.22) show that, at early times, $t \ll (p_0/T)t_{\text{rel}}$, there is a remnant of the original perturbation — the ‘jet front’ localized at $z = t$, as described by the first term in the r.h.s. of Eq. (4.21) — whose momentum distribution is however degrading with time, in the same way as in Eq. (4.24). With increasing time, this ‘jet front’ is gradually washed out and a new distribution develops around $p = 0$, which is slowly varying in z (for $|z| \ll t$ at least). For sufficiently large times, $t \gg (p_0/T)t_{\text{rel}}$, and sufficiently far behind the front, $z \lesssim t - t_{\text{rel}}$, this new distribution is thermal in p :

$$f_G(t, z, p; p_0) \simeq \frac{e^{-|p|}}{2} \frac{e^{-\frac{(z-p_0)^2}{4t}}}{2\sqrt{\pi t}} \quad \text{when } t \gg p_0 \gg 1 \text{ and } |z| \ll t. \quad (4.27)$$

This is recognized as the product between the Maxwell-Boltzmann distribution in momentum, cf. Eq. (4.26), and the one-dimensional heat kernel describing diffusion in z . Eq. (4.27) shows that the large-time distribution is centered around $z = (p_0/T)t_{\text{rel}}$ (the maximal distance travelled by the original perturbation until it has lost all its energy, due to drag) and that its longitudinal extent grows with time, according to $\Delta z(t) \simeq \sqrt{4t_{\text{rel}}t}$. Thus, remarkably, the momentum–space diffusion originally encoded in the Fokker–Planck equation has also generated *spatial* diffusion. One may chose as a criterion for having a quasi-homogeneous distribution the condition that the longitudinal extent

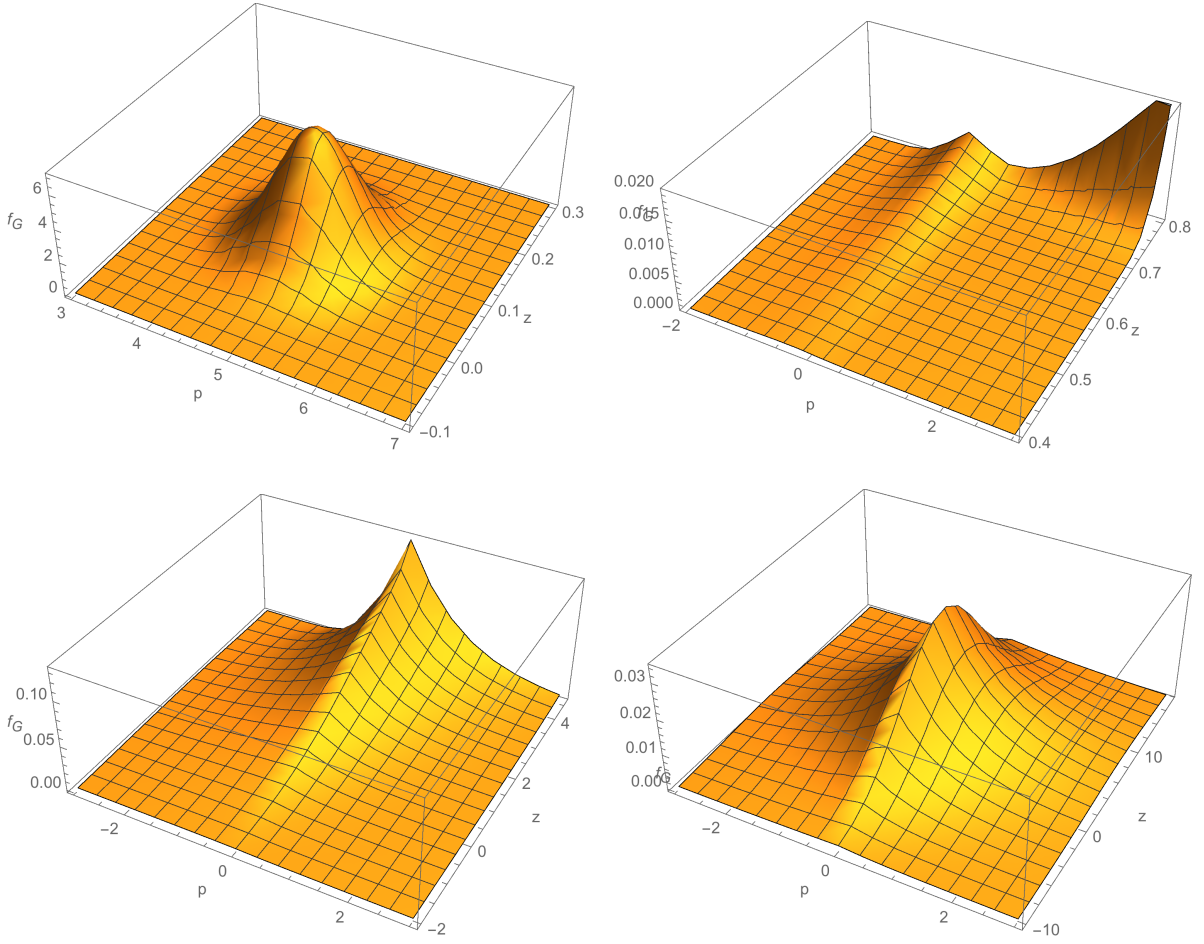


Figure 5. The Green's function in Eqs. (4.21)–(4.22) plotted as a function of p and z for $p_0 = 5$ and four values of t : upper line, left: $t = 0.1$; upper line, right: $t = 1$; lower line, left: $t = 5$; lower line, right: $t = 20$. Note that the vertical scales and also the ranges in p and z can significantly differ from one figure to another. For $t \gtrsim 1$, one can see the emergence and growth of a thermal tail at $|z| \ll t$, which for $t \gg p_0$ is the Gaussian shown in Eq. (4.27).

$\Delta z(t)$ be larger than the location $(p_0/T)t_{\text{rel}}$ of the center. This happens for

$$t \gtrsim \frac{1}{4} \left(\frac{p_0}{T} \right)^2 t_{\text{rel}}, \quad (4.28)$$

a time scale considerably larger than that required by the thermalization of the momentum distribution. Note finally that by integrating Eq. (4.27) over z and over p we recover, to the accuracy of interest, the normalization of the initial perturbation, i.e. $\int dz dp f_G(t, z, p) = 1$, which confirms that the whole perturbation has thermalized. If on the other hand one computes the total energy contained in the thermalized distribution (4.27) one finds, clearly, $\int dz dp |p| f_G(t, z, p) \simeq T$ for $t \gg (p_0/T)t_{\text{rel}}$. That is, out of the total energy $p_0 > T$ of the original perturbation, a fraction T/p_0 is carried at large times by the thermalized distribution, whereas the remaining fraction $(p_0 - T)/p_0$ has been transmitted to the medium, via drag. This conclusion on the energy loss is similar to our previous findings for the case of a stationary source in Sect. 4.1.

4.2.2 A physical source generated by the branching process

In this subsection we apply the Green’s function method to the main physical problem of interest, namely a source generated by a branching process. More precisely, we consider an *ideal* branching process, for which the splitting dynamics at $p > p_*$ is not at all influenced by elastic collisions: the medium solely acts as a ‘perfect sink’ which absorbs the energy of the gluon cascade at the ‘infrared’ scale $p_* \sim T$. (A more general situation will be studied in Sect. 5.) Under these circumstances, the source has the structure shown in Eq. (4.2) with $\Gamma(t, p_*) = \mathcal{F}(E, p_*, t)/p_*$. Here, $\mathcal{F}(E, p_*, t)$ is the energy flux at p_* generated at time t by a cascade that was initiated at $t = 0$ by a leading particle with initial energy $E \gg T$ (recall the discussion in Sect. 2.1). This source truly represents a bunch of relatively soft particles, which carry all the same energy p_* , move together at the speed of light, and whose number is evolving in time due to the branching dynamics.

Within the context of the ideal cascade, one was able to obtain an exact analytic result for this function $\mathcal{F}(E, p_*, t)$ [28]. Strictly speaking, the analysis in [28] required two additional assumptions, which are not essential from the viewpoint of physics, but simplify the mathematical manipulations:

(a) the energy E of the LP is not *too* large, namely it obeys⁹ $E \leq \omega_c(L) \equiv \hat{q}L^2$, where the upper limit $\omega_c(L) = \omega_{\text{br}}(L)/\bar{\alpha}^2$ is parametrically larger than $\omega_{\text{br}}(L)$ at weak coupling;

(b) the kernel (3.7) within the BDMPSZ splitting rate is replaced by its simplified version $\mathcal{K}_0(x) \equiv 1/[x(1-x)]^{\frac{3}{2}}$, which preserves the correct behavior near the singular endpoints at $x = 0$ and $x = 1$.

Under these assumptions, the energy flux is obtained as [28]

$$\mathcal{F}(E, p_*, t) = 2\pi E \frac{t}{t_{\text{br}}^2(E)} e^{-\pi t^2/t_{\text{br}}^2(E)} = \frac{d}{dt} \Delta E_{\text{flow}}, \quad (4.29)$$

where $t_{\text{br}}(E)$ is the branching time introduced in Eq. (2.5) (the typical time after which a parton with energy E undergoes the first democratic branching) and

$$\Delta E_{\text{flow}}(E, p_*, t) = E [1 - e^{-\pi t^2/t_{\text{br}}^2(E)}] = E [1 - e^{-\pi \omega_{\text{br}}(t)/E}] \quad (4.30)$$

with $\omega_{\text{br}}(t) = \bar{\alpha}^2 \hat{q} t^2$, is the energy which accumulates into the soft modes with $p \leq p_*$ after a time t . The above results strictly apply for $p_* \ll \omega_{\text{br}}(t)$, or, equivalently $t \gg t_{\text{br}}(p_*) \sim t_{\text{rel}}$, and within that regime they are independent of p_* . In fact, in the absence of the sink at p_* , this whole energy would accumulate in a condensate at $p = 0$ [28].

Eq. (4.30) confirms that the time scale $t_{\text{br}}(E)$ plays the role of the lifetime of the leading particle w.r.t. democratic branchings. At small times $t \ll t_{\text{br}}(E)$, one can expand the exponential there to lowest order and thus find

$$\Delta E_{\text{flow}}(t) \simeq \pi \omega_{\text{br}}(t) \quad \text{when } t \ll t_{\text{br}}(E). \quad (4.31)$$

Alternatively, this estimate is correct for a given time t provided the energy E of the LP is sufficiently high, $E \gg \omega_{\text{br}}(t)$. This result is in agreement with (2.6) up the replacement $v \rightarrow 2\pi$, due to the use of the approximate kernel $\mathcal{K}_0(x)$. It shows that, at small times, the energy loss via flow is independent of E (essentially, because the LP does not ‘feel’ the change in its own energy due to flow) and that it grows with time like t^2 . As explained in Sect. 2, this ‘small time’ (or ‘high energy’) regime is the most interesting one for jets at the LHC, where one indeed has $E \gg \omega_{\text{br}}(L)$, with L the size of the medium.

⁹The generalization of the subsequent results to more energetic jets with $E \gg \omega_c(L)$ can be found in Ref. [30].

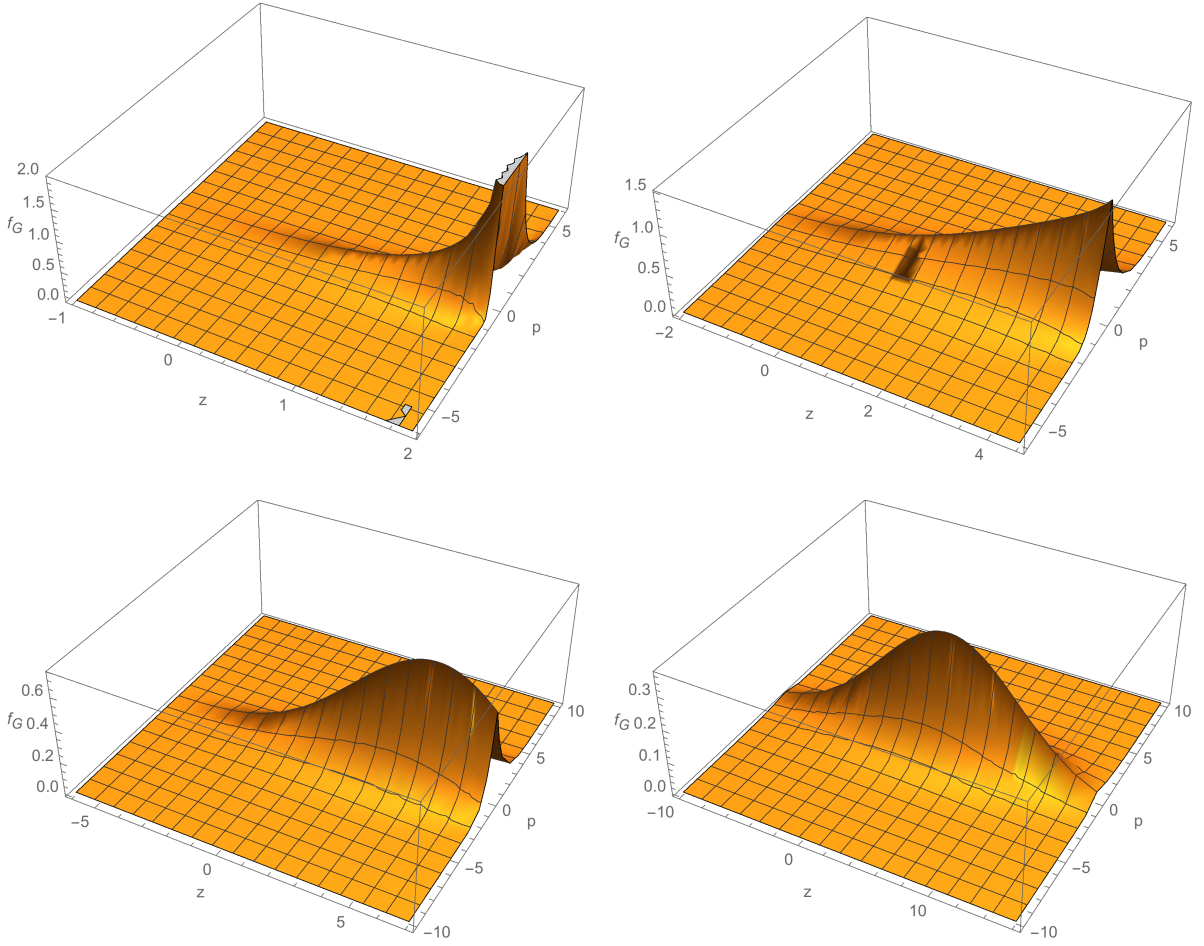


Figure 6. The distribution (4.32) produced by the source in Eq. (4.29) with $t_{\text{br}}(E) = 6$ and $p_* = 1$ is plotted as a function of p and z for four values of t : upper line, left: $t = 2$; upper line, right: $t = 5$; lower line, left: $t = 8$; lower line, right: $t = 20$. For relatively small times $t < t_{\text{br}}(E)$, the source is still active and the distribution is thermal only in the tail at $z < t - t_{\text{rel}}$. For larger times $t > t_{\text{br}}(E) + p_*$, the source has essentially decayed and the distribution is thermal at any z . For $t = 20$ there is no significant difference between the exact result displayed above and the respective prediction of the diffusion approximation (4.33).

For larger times, such that $t \sim t_{\text{br}}(E)$ or, equivalently, $E \sim \omega_{\text{br}}(t)$, the LP disappears via democratic branching and its whole initial energy is carried away by the flow. This is indeed consistent with Eq. (4.31) which shows that $\Delta E_{\text{flow}}(t) \simeq E$ when $t \gtrsim t_{\text{br}}(E)$. From a physical viewpoint, this ‘large time’ (or ‘low energy’) regime better corresponds to the primary gluons radiated by the LP, which evolve into ‘mini-jets’.

It is also interesting to notice the time dependence of the energy flux in Eq. (4.29): this rises linearly with t at small times, then reaches a maximal value around $t = t_{\text{br}}(E)$, and rapidly vanishes at larger times. This means that the production rate for soft gluons is largest towards the late stages of the branching process, i.e. for $t \sim t_{\text{br}}(E)$, just before the LP dies away.

We now return to the solution to the Fokker–Planck equation for the physical source at hand.

Using Eq. (4.2), the integrals over z_0 and p_* in Eq. (4.15) can be immediately performed to yield

$$f(t, z, p) = \frac{1}{p_*} \int_0^t dt' f_G(t - t', z - t', p; p_*) \mathcal{F}(t'). \quad (4.32)$$

It seems difficult to analytically perform the remaining integral over t' , but this can be numerically computed, with the results shown in Fig. 6 (in terms of reduced variables¹⁰). These results can be understood as follows: For relatively small times, $t \ll t_{\text{br}}(E)$, the source (the leading particle) is still present and the gluon distribution is quite similar to that produced by a stationary source, as shown in Fig. 3: it exhibits a front at $z = t$ and $0 < p < p_*$ (but with the edges smeared out by diffusion), which represents the gluons that have been recently emitted, and with a tail at $z < t$ and peaked in momentum at $p = 0$, which describes the gluons which have experienced the effects of collisions. For later times $t \gtrsim t_{\text{br}}(E)$, the source has disappeared via democratic branching and the gluon distribution looks quite similar to that produced by a localized source at late times, cf. Fig. 5: a thermal distribution in momentum which extends in z via diffusion and which peaks around $z = t_{\text{br}}(E)$ (the maximal displacement of the source before it dies away).

In fact, for sufficiently large time, $t - t_{\text{br}}(E) \gg (p_*/T)t_{\text{rel}} \sim t_{\text{rel}}$, one can use the diffusion approximation for the Green's function, Eq. (4.27), to deduce (in reduced variables, cf. footnote 10)

$$f(t, z, p) \simeq 4\pi\bar{\alpha}^2 \frac{e^{-|p|}}{p_*} \int_0^t dt' t' \frac{e^{-\frac{(z-t')^2}{4(t-t')}}}{\sqrt{4\pi(t-t')}} e^{-\pi t'^2/t_{\text{br}}^2(E)}. \quad (4.33)$$

This represents the medium perturbation that would be left over by a relatively soft mini-jet ($E \ll \omega_{\text{br}}(t)$), after it thermalizes. By integrating this late-time distribution over z and p , it is easy to check that it encompasses all the particles generated by the source, $\int dz dp f(t, z, p) = E/p_*$, as it should, and that it contains a fraction T/p_* of the total energy:

$$\Delta E_{\text{ther}} = \int dz dp |p| f(t, z, p) \Big|_{\text{large time}} \simeq \frac{T}{p_*} E \quad \text{when } t \gg t_{\text{br}}(E). \quad (4.34)$$

We thus conclude that by choosing $p_* = T$ one can ensure that the whole initial energy of the source is eventually recovered in the thermalized gluon distribution: the energy loss via viscous drag is negligible since the gluons are directly injected at the thermal scale.

5 Numerical studies of the kinetic equation

The general discussion and the parametric estimates for the energy loss presented in Sect. 2, as well as the explicit calculations using the Green's function method in Sect. 4.2.2, were based on an important physical assumption: the fact that the gluon cascade generated via multiple branchings is not modified by the elastic collisions responsible for thermalization and hence it can be modeled as an ideal branching process, along the lines of Refs. [28, 30] — that is, a turbulent cascade, for which the medium acts as a perfect sink at the lower end ($p \sim T$) of the cascade. The validity of this assumption is far from being obvious, as shown by the following argument: via elastic collisions, the soft gluons

¹⁰ When rewriting Eq. (4.1) in terms of reduced variables, we find that the dimensionless version of the source in Eq. (4.2) reads (we restore the hat on reduced quantities, for more clarity): $\hat{S} = \theta(\hat{t})\delta(\hat{t} - \hat{z})\delta(\hat{p} - \hat{p}_*)(\hat{\mathcal{F}}/\hat{p}_*)$, where $\hat{\mathcal{F}} \equiv \mathcal{F}/T^2 = 8\pi\bar{\alpha}^2\hat{t} \exp\{-\pi\hat{t}^2/\hat{t}_{\text{br}}^2(E)\}$ depends upon the energy E only via the reduced branching time $\hat{t}_{\text{br}}(E) \equiv t_{\text{br}}(E)/t_{\text{rel}}$.

are redistributed in phase space, in such way to match a thermal distribution, and for $p \sim T$ the latter is quite different from the scaling spectrum produced by the turbulent cascade.

In this section, we shall give up the ‘perfect sink’ assumption and present a detailed numerical study based on the kinetic equation (3.10). This equation too is a rather simplified version of the actual dynamics, as explained in Sect. 3, but as compared to the source approximation in Sect. 4 it has the merit to include an explicit infrared cutoff $p_* \sim T$ in the branching process and also the interplay between branching and thermalization at $p > p_*$.

5.1 Setting-up the problem

As in the previous section, it is convenient in practice to measure all the momenta in units of T and all the space-time scales in units of t_{rel} , that is, to use the reduced variables introduced in Eq. (4.3). In terms of these variables, the kinetic equation (3.10) reads (with $v \equiv p/|p|$)

$$\begin{aligned} (\partial_t + v\partial_z) f(t, z, p) &= \partial_p(\partial_p + v)f(t, z, p) \\ &+ \frac{t_{\text{rel}}}{t_{\text{br}}(T)p^{\frac{1}{2}}} \int_r dx \mathcal{K}(x) \left[\frac{1}{\sqrt{x}} f\left(t, z, \frac{p}{x}\right) - \frac{1}{2} f(t, z, p) \right], \end{aligned} \quad (5.1)$$

where we recall that the subscript r on the integral over x indicates the condition that both daughter gluons in a splitting process be harder than the ‘infrared’ scale $p_* \sim T$ (the lower end of the cascade). The precise kinematical conditions are as follows: for the gain term, $p > p_*$ and $p(1-x)/x > p_*$, whereas for the loss term, $xp > p_*$ and $(1-x)p > p_*$. For definiteness, we chose this scale p_* to be exactly equal to T (i.e. $p_* = 1$ in Eq. (5.1)).

The ratio $t_{\text{rel}}/t_{\text{br}}(T)$ which appears in front of the branching term in Eq. (5.1) is parametrically of order one for the weakly-coupled quark-gluon plasma. For what follows, it is convenient to choose this ratio to be *exactly* equal to one. This choice is also reasonable from a physics standpoint: it corresponds to the condition $\hat{q} = 16\bar{\alpha}^2 T^3$ (or, equivalently, $4\bar{\alpha}^2 T t_{\text{rel}} = 1$), which is satisfied by the following values for the physical parameters:

$$\bar{\alpha} = 0.3, \quad T = 0.5 \text{ GeV}, \quad \hat{q} = 1 \text{ GeV}^2/\text{fm} \simeq 0.2 \text{ GeV}^3, \quad t_{\text{rel}} = 1 \text{ fm}, \quad (5.2)$$

which are indeed consistent with the current phenomenology.

The equation thus obtained will be solved numerically, with the initial condition

$$f(t=0, z, p) = \delta(p-E)\delta(z) \rightarrow \frac{10}{\pi} e^{-10(p-E)^2 - 10z^2}, \quad (5.3)$$

where the product of δ -functions is regulated as shown in the r.h.s. The picture that we expect in the light of the general discussion in Sect. 2 is as follows:

(i) For sufficiently small times $t \ll t_{\text{br}}(E)$, the leading particle should survive and carry most of the total energy. The energy lost towards the medium should be comparatively small and follow the law shown in Eq. (2.6); that is, it should be of order $\omega_{\text{br}}(t)$ and thus grow with t as t^2 .

(ii) For larger times $t \gtrsim t_{\text{br}}(E)$, the LP should disappear via democratic branching and the energy loss should be of the order of the total energy E .

For what follows, one should keep in mind that some of the assumptions underlying this picture might not be well satisfied when solving Eq. (5.1) in practice. For instance, in Sect. 2 we have assumed

the medium to act as a perfect sink for the energy carried away by the branching process, which in turn allowed for a well-developed phenomenon of turbulence. This is an important hypothesis, implicitly assumed in the previous literature, for which our subsequent study will provide an explicit test.

5.2 The gluon spectrum

Before we describe the full picture of the gluon cascade in the longitudinal phase-space (z, p) , let us present the results for the distribution integrated over z , that is, the gluon spectrum

$$f(t, p) \equiv \frac{dN_g}{dp} = \int dz f(t, z, p). \quad (5.4)$$

Clearly, this function can be obtained by solving directly the homogeneous (in the sense of independent of z) version of Eq. (5.1), with initial condition $f(0, p) = \delta(p - E)$. This is a relatively simple numerical problem, which in particular allows for an extensive study of the role of the lower cutoff at $p = p_*$ on the branching process. To that aim, we shall consider three cases: (a) an ‘ideal’ branching process, which involves no infrared cutoff and develops a clear phenomenon of turbulence (the corresponding equation is obtained by keeping only the branching term in the r.h.s. of Eq. (5.1) and letting $p_* = 0$); (b) a branching process with a sharp infrared cutoff at $p_* \ll E$, as described by Eq. (5.1) without the Fokker-Planck terms, and (c) the complete dynamics (branchings with infrared cutoff p_* and elastic collisions), as described by the homogeneous version of Eq. (5.1).

As already mentioned, the ideal branching process has been extensively studied in the literature and, in particular, exact analytic solutions have been obtained [28] for the case of a simplified kernel $\mathcal{K}(x) \rightarrow \mathcal{K}_0(x) \equiv 1/[x(1-x)]^{\frac{3}{2}}$. In our numerical study, we use the full kernel in Eq. (3.7), but the solution is qualitatively similar to that presented in Ref. [28]. Namely, for sufficiently small momenta $p \ll E$, the spectrum exhibits the scaling law $f(t, p) \propto 1/p^{3/2}$, which is a fixed point of the branching kernel and the signature of wave turbulence. For not too large times $t \ll t_{\text{br}}(E)$, the leading particle is visible in the spectrum, as a pronounced peak just below $p = E$. The width of this peak increases with time (due to radiation) and eventual becomes of order one — meaning that the LP undergoes its first democratic branching — when $t \sim t_{\text{br}}(E)$. For even larger times, the scaling law $\sim 1/p^{3/2}$ is still visible at small p , but the spectrum is suppressed as a whole, since the energy flows via multiple branching and accumulates at $p = 0$. When $t \gg t_{\text{br}}(E)$, the whole energy E ends up in this ‘condensate’. This behavior is clearly visible in the numerical results displayed in Fig. 7.

After introducing the infrared cutoff p_* , the gluons with $p \leq 2p_*$ cannot split anymore, as there is no phase-space available to the daughter gluons. Hence, instead of falling at $p = 0$, gluons start accumulating in the bins at $p \gtrsim p_*$. As a result, the spectrum above p_* deviates from the scaling spectrum: it shows an excess (‘pile-up’), which is particularly marked at $p_* < p < 2p_*$, where it looks like a bump. Both the size of this excess and its extent in p above p_* are increasing with time, as clearly visible in Fig. 7. This can be understood as follows: a gluon with, say, $p = 3p_*$ has more chances to be created via the decay of parent gluons with $p \gg p_*$ (for which the kinematical constraint is relatively unimportant) than to disappear via a decay (since a significant fraction of the phase-space for its decay, that at $p \leq p_*$, is not accessible anymore).

On physical grounds, it is quite clear that this pile-up cannot be entirely physical: gluons with $p \sim T$ can efficiently lose energy towards the medium via elastic collisions and hence they should fall into the bins at lower energies $|p| < T$. We thus expect the pile-up to be considerably reduced and possibly washed out after also including the elastic collisions, as represented by the Fokker-Planck

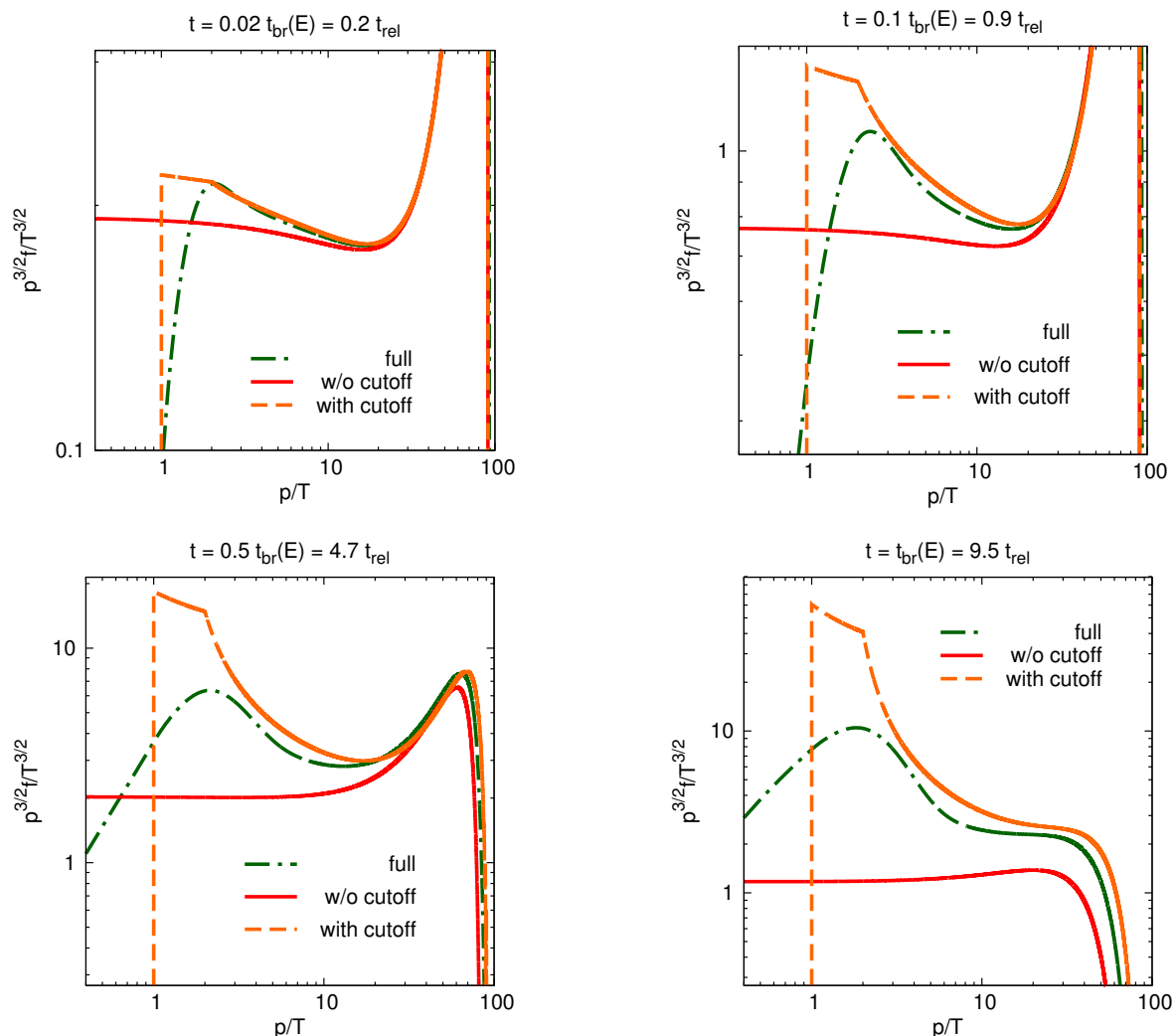


Figure 7. The gluon spectrum $f(t, p)$ for a spatially homogeneous distribution, for an initial energy $E = 90T$ and 4 values of time. The three curves correspond to (a) an ideal branching process (the red, continuous, line), (b) a branching process with infrared cutoff $p_* = T$ (orange, dotted line), and (c) the full process with branchings and elastic collisions (green, dashed-dotted line). On the vertical axis, the spectrum is multiplied by $(p/T)^{3/2}$ to render manifest the scaling behavior for the ideal branching process.

terms in the r.h.s. of Eq. (5.1). This expectation is confirmed by the numerical solution to the homogeneous version of Eq. (5.1) (whose results are shown too in Fig. 7), but only partially: the pile-up in the spectrum is indeed reduced by the elastic collisions, but the deviation with respect to the scaling spectrum remains quite large — so large, that there seems to be no scaling window in practice. If true, the last conclusion would also imply that the physical results are very sensitive to the details of the mechanism which stops the branching process and which in our analysis has been only crudely mimicked by the infrared cutoff p_* . Fortunately though, these last conclusions are not fully right and the numerical results exhibited in Fig. 7 are in this respect quite misleading. The gluons which appear to accumulate on top of the scaling spectrum in this figure are actually located at *different* values of z . These are relatively soft gluons, which undergo strong diffusion as a consequence of collisions and thus separate from each other and also from the more energetic constituents of the jet (which keep

propagating along the light-cone at $z = t$). Hence the ‘pile-up’ visible in the curves denoted as ‘full’ in Fig. 7 is merely an artifact of integrating the gluon distribution over the longitudinal coordinate z : it comes from the superposition of a nearly ideal branching spectrum in the front of the jet at $z \simeq t$ and of nearly thermal spectra in the tail of the jet at $z \ll t$. This will be demonstrated by the subsequent analysis, where the z -distribution is kept explicit.

5.3 Jet evolution in longitudinal phase-space

In this subsection we present numerical solutions to the complete equation (5.1) with initial conditions of the type shown in Eq. (5.3). We consider two values for the initial energy, $E = 25T$ and $E = 90T$, which correspond to rather distinct physical situations. The first value $E = 25T$ ($= 12.5$ GeV according to Eq. (5.2)) is quite low and is representative for a *mini-jet* radiated by a leading particle with a much higher energy $E_0 \geq 100$ GeV. This is one of the typical mini-jets which control the energy loss in the case where the LP crosses the medium along a distance $L \simeq t_{\text{br}}(E) = 5 t_{\text{rel}} = 5$ fm. The second value $E = 90T = 45$ GeV is closer to the energy of an actual jet at the LHC and in particular is large enough to ensure that the respective leading particle does not disappear into the medium: indeed, the respective branching time $t_{\text{br}}(E) \simeq 9.5$ fm is larger than the typical distance $L \lesssim 8$ fm that the LP might travel across the medium in the experimental situation at the LHC.

5.3.1 The gluon distribution and the energy density

The general features of the evolution of the gluon cascade produced by a high-energy jet can be appreciated by inspection of Figs. 8 and 9, which show the phase-space distribution of the gluon number $f(t, z, p)$ and, respectively, the gluon energy $|p|f(t, z, p)$, for the two energies of the LP, $E = 90T$ and $25T$, and four values of time: $t/t_{\text{rel}} = 0.95, 4.7, 9.5$, and 14 . These particular values for t have been chosen since, with our present conventions (i.e. $t_{\text{br}}(E)/t_{\text{rel}} = \sqrt{E/T}$), they correspond to rather special values for the case of a jet with $E = 90T$; namely, they amount to $t/t_{\text{br}}(90) \simeq 0.1, 0.5, 1$, and 1.5 , respectively. Since the natural time scale for the jet evolution is $t_{\text{br}}(E)$, let us also list the corresponding values for the softer jet with $E = 25T$: one roughly has $t/t_{\text{br}}(25) \simeq 0.2, 1, 2$, and 3 , respectively. To gain more intuition about these time scales in physical units, it is useful to recall that $t_{\text{rel}} = 1$ fm for the medium parameters in Eq. (5.2).

When discussing Figs. 8 and 9, it is natural to group together those plots which correspond to different values of the energy E , but similar values of $t/t_{\text{br}}(E)$, because they refer to similar stages in the evolution of the jet via branching. But even for identical values of $t/t_{\text{br}}(E)$, one should still expect some differences between the two cases, $E = 90T$ and $E = 25T$, because the physics of thermalization introduces an additional energy scale in the problem — the infrared cutoff p_* .

Consider first Figs. 8 (a)-(c) and Figs. 9 (a)-(c), which illustrate the evolution at early stages, $t < t_{\text{br}}(E)$. Figs. 8 (a)-(c) show that, already for such early times, most of the particles are relatively soft ($p \sim p_* = T$), meaning that they are products of radiation. In particular, those particles which at a given time t have an energy $|p|$ smaller than $\omega_{\text{br}}(t) = \bar{\alpha}^2 \hat{q} t^2$, are generally produced via *multiple branchings*, that is, they belong to gluon cascades generated via democratic branchings by primary gluons with $p \sim \omega_{\text{br}}(t)$. But so long as $t \ll t_{\text{br}}(E)$, most of the energy is still carried by the LP, as manifest in Figs. 9 (a)-(b): the energy distribution is peaked at a value which is smaller than, but comparable to, the original energy E . When $t_{\text{rel}} \lesssim t \ll t_{\text{br}}(E)$, the energy loss by the LP and its longitudinal broadening are both controlled by soft branchings and hence they grow with time like t^2 .

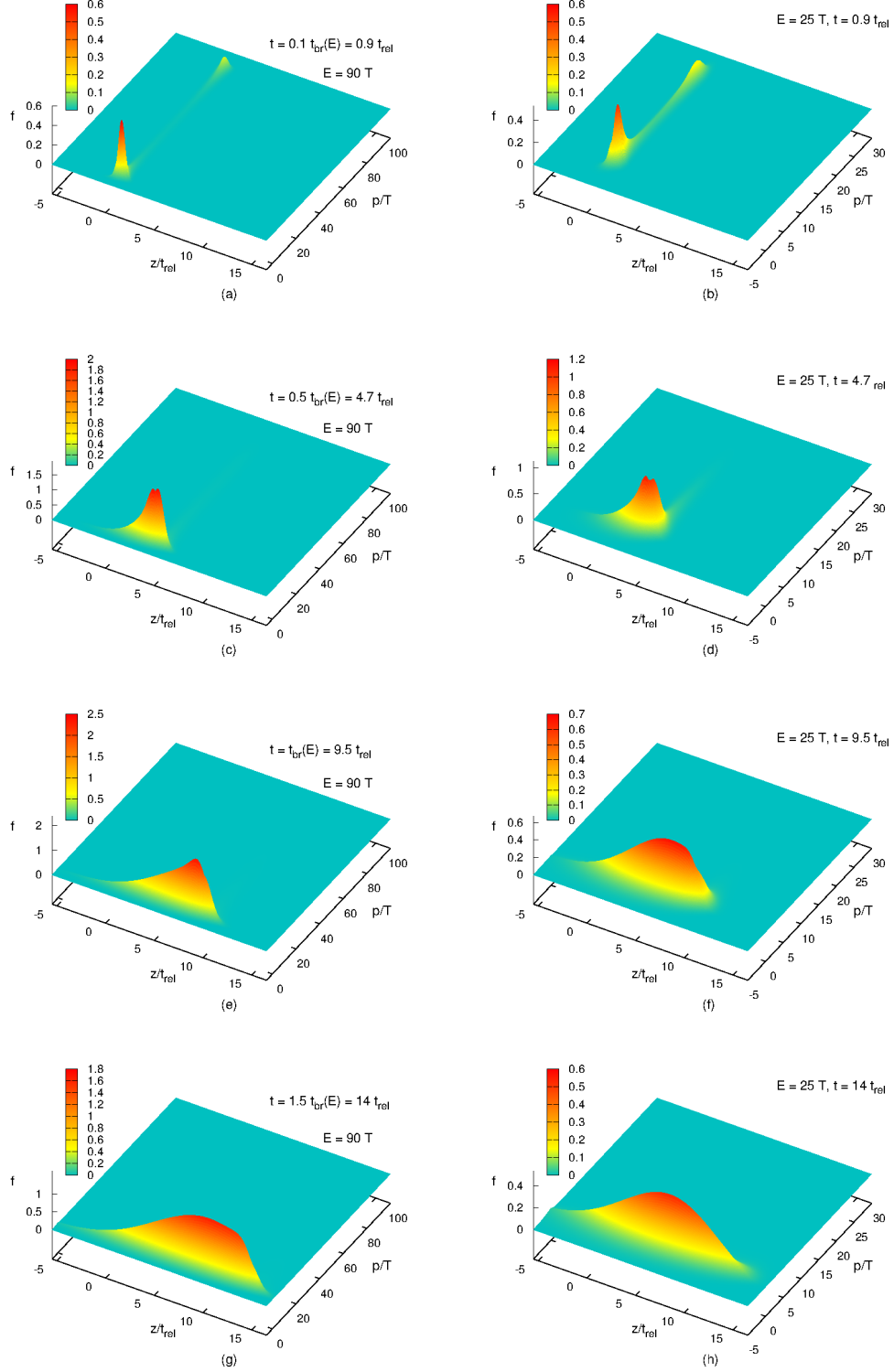


Figure 8. The time evolution of the phase-space distribution $f(t, z, p)$ produced by a jet with initial energy $E = 90 T$ (left) and respectively $E = 25 T$ (right), plotted for exactly the same values of time.

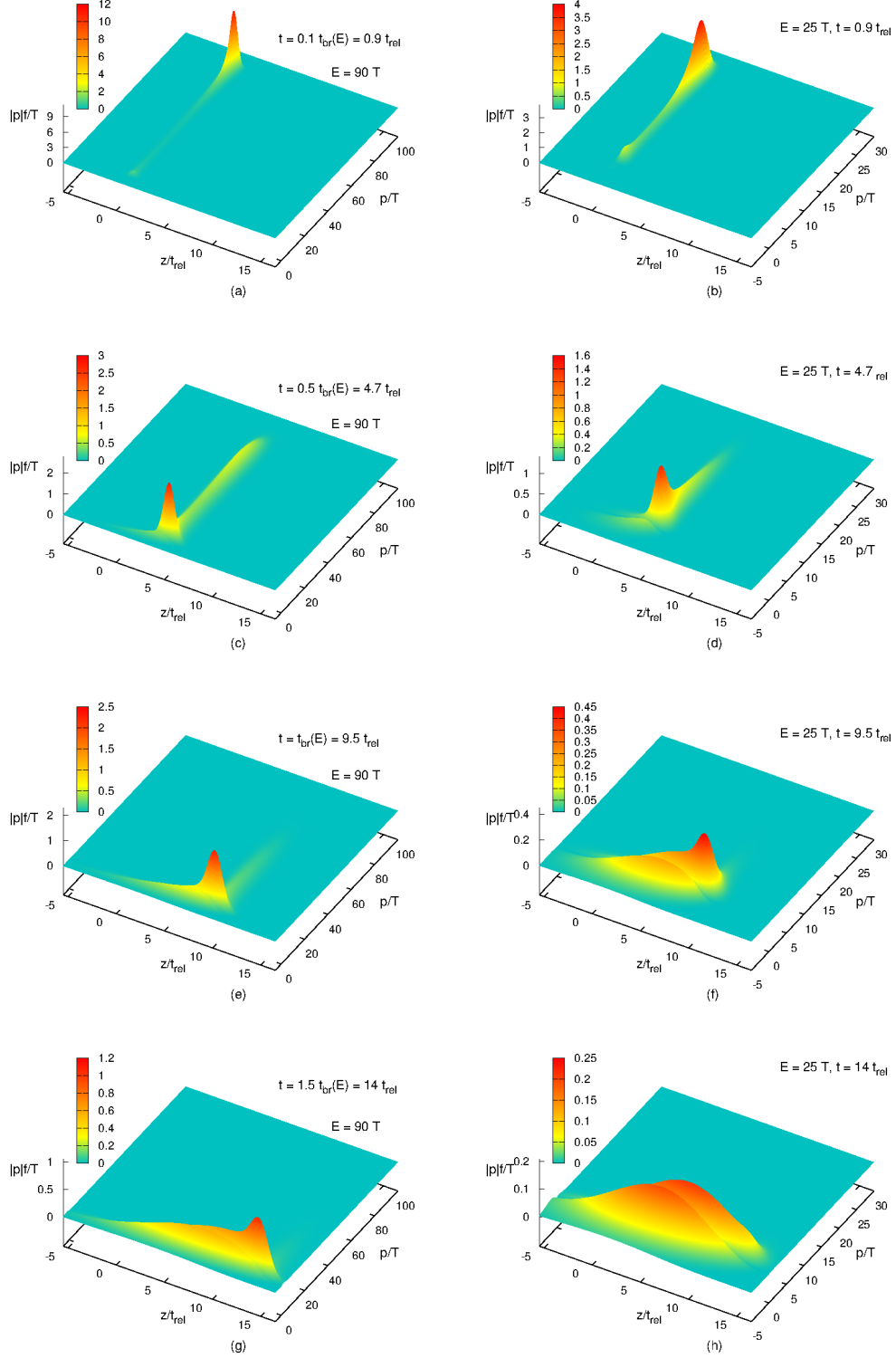


Figure 9. The time evolution of the phase-space energy density $|p|f/T$, for the same conditions as in Fig. 8.

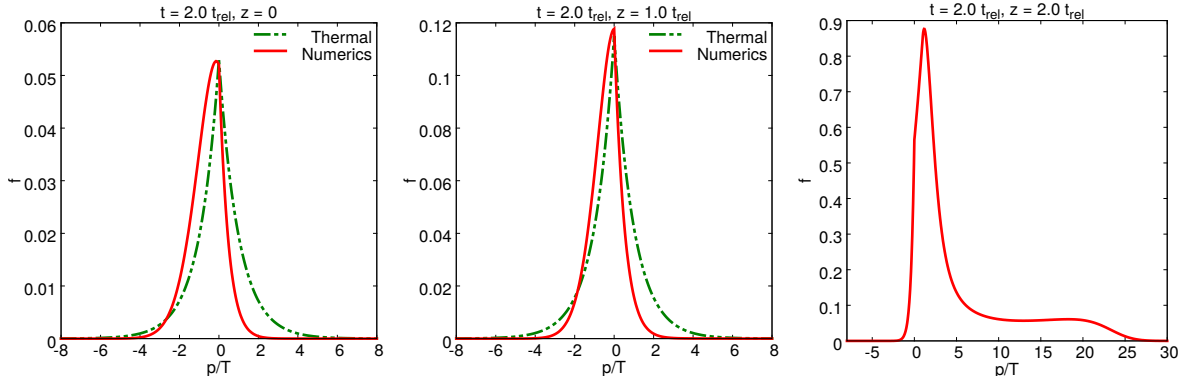


Figure 10. The gluon distribution $f(t, z, p)$ for $E = 25T$ is represented as a function of p at time $t = 2t_{\text{rel}}$ and for 3 different values of z : $z = 0$, $z = t_{\text{rel}}$, and $z = 2t_{\text{rel}}$. For $z < t - t_{\text{rel}}$, the momentum distribution is nearly thermal, but with an overall strength which depends upon z : $f(z, p) \simeq f_0(z)e^{-|p|/T}$. For $z = t$ on the other hand, the distribution is far from thermal equilibrium, albeit it is still strongly peaked near $p = T$. Similar conclusions hold for the distribution at later times and for a jet with $E = 90T$.

Fig. 9 (c) shows another interesting feature: for $t \simeq 0.5t_{\text{br}}(E)$, one sees a second peak emerging in the energy distribution at $p \sim T$. This demonstrates the strong accumulation of gluons towards the lower end of the spectrum which in turn reflects a limitation of the medium capacity to act as a ‘perfect sink’. We shall later return to a more detailed study of this phenomenon (see notably Figs. 11 and 14 and the associated discussions).

As also visible in Figs. 8 (a)-(c), the approach to thermalization in the tail of the distribution at $z < t$ is noticeable already at such early times $t < t_{\text{br}}(E)$. There is indeed a substantial number of gluons which remain behind the LP (i.e., which do not travel at the speed of light) and whose momentum distribution is nearly thermal. This is more clearly illustrated by the plots in Fig. 10, corresponding to $E = 25T$, which show the momentum distribution at $t = 2t_{\text{rel}} = 0.4t_{\text{br}}(25)$ and for different values of z : the shape of this distribution is close to the exponential $e^{-|p|/T}$ at any $z \lesssim t - t_{\text{rel}}$.

Consider now later times $t \gtrsim t_{\text{br}}(E)$, where one expects the LP to disappear via democratic branching. Figs. 9 (d) and (e) confirm that, when $t \sim t_{\text{br}}(E)$, there is no visible trace of the LP, albeit a few semi-hard particles, with $T \ll p \ll E$, still exist. For even larger times, these semi-hard particles will themselves disappear via democratic branchings, so there will be an increasing fraction of the total energy which is carried by the soft gluons with $p \lesssim T$. This trend is indeed visible in Figs. 9 (f)-(h). However, one should not conclude that all this energy has already thermalized: the soft gluons which propagate together with their (semi-)hard sources along the light-cone $z = t$ cannot be thermal. This is already illustrated by the last plot in Fig. 10: the momentum distribution corresponding to $z = t = 2t_{\text{rel}}$ is peaked at small $p \sim T$, yet it strongly deviates from a thermal distribution.

To better distinguish between thermal and non-thermal (soft) gluons at late times, we have exhibited in Fig. 11 the z -distribution of the energy and number densities, defined as

$$\varepsilon(t, z) = \int dp |p| f(t, z, p), \quad n(t, z) = \int dp f(t, z, p). \quad (5.5)$$

As visible in these plots, even for times as large as $t = 1.5t_{\text{br}}(E)$, where we know (say, from Figs. 9 (f) and (g)) that the energy is preponderantly carried by soft quanta with $p \sim T$, the energy distribution

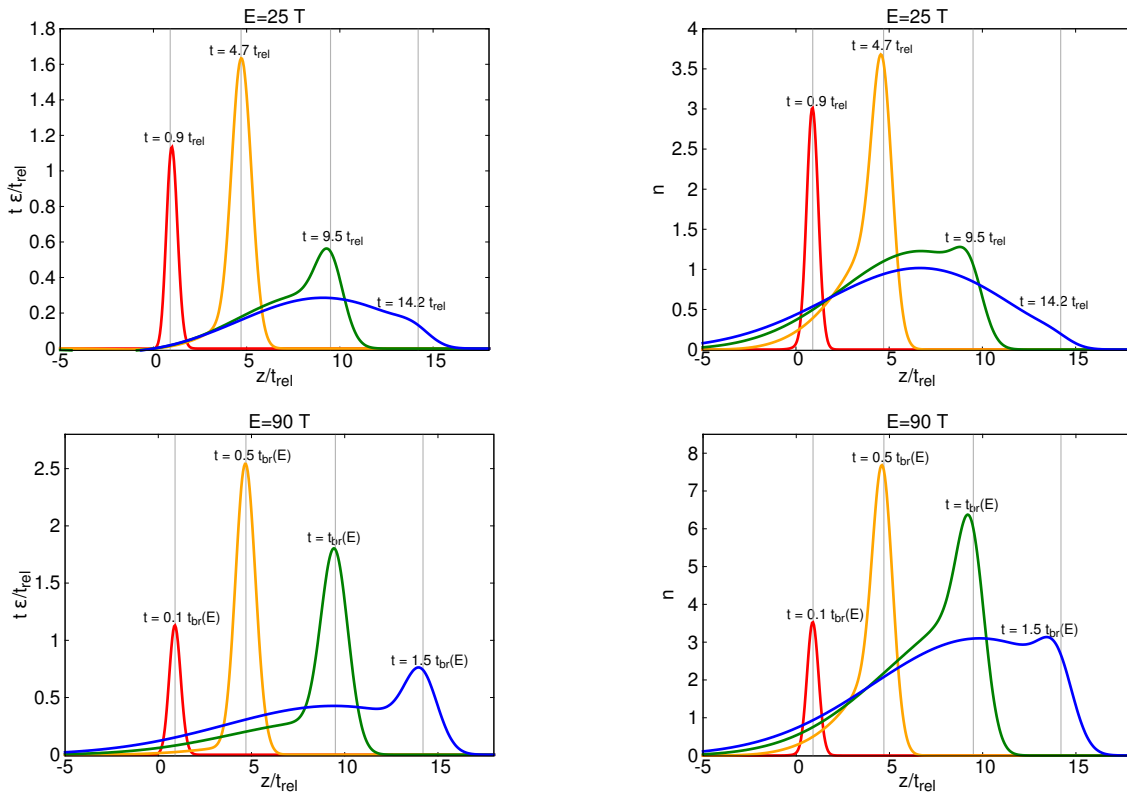


Figure 11. The energy density and the gluon number density are shown as functions of z at different times. The grey vertical lines indicate the location of the light-cone, that is, $z = t$, for each value of t .

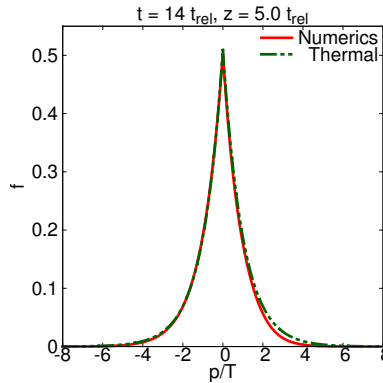


Figure 12. The gluon distribution $f(t, z, p)$ for $E = 25 T$ is plotted as a function of p for $t = 14.2 t_{\text{rel}} \simeq 3 t_{\text{br}}(E)$ and $z = t_{\text{br}}(E) = 5 t_{\text{rel}}$ and compared to a thermal distribution with the same normalization at $p = 0$.

is still strongly peaked at $z = t$, meaning that most of these soft gluons are *not* thermal: they have been emitted at late stages and did not have the time to thermalize. This finding is in agreement with the discussion following Eq. (4.29), where we noticed that the flux of soft gluons is largest towards the late stages of the cascade. The situation changes at the larger time $t = 3 t_{\text{br}}(E)$, that we can here access only for the jet with $E = 25 T$ (by looking at $t = 14.2 t_{\text{rel}} \simeq 3 t_{\text{br}}(25)$). In that case, we see

that both densities, $\varepsilon(t, z)$ and $n(t, z)$, peak well behind the light-cone — in particular, the number distribution peaks around $z \simeq t_{\text{br}}(E) = 5 t_{\text{rel}}$, in agreement with Eq. (4.33). This strongly indicates that the entire gluon distribution produced by the jet has thermalized by $t = 3 t_{\text{br}}(E)$: the jet is *fully quenched*. This conclusion can be also checked by plotting the distribution $f(t, z, p)$ as a function of p for $t = 3 t_{\text{br}}(E)$ and, say, $z = t_{\text{br}}(E)$: this is shown in Fig. 12 which indeed features an almost perfect thermal distribution. The distribution of such a fully quenched jet in longitudinal phase-space is illustrated by Figs. 8 (h) and 9 (h). Clearly, this is very similar to the late-time distributions found in Sect. 4, cf. Figs. 5 and 3: a distribution symmetric in z which extends via diffusion.

5.3.2 Energy loss towards the medium

Given our numerical results, as presented in the previous subsection, it is furthermore interesting to use them to extract the energy lost by the jet towards the medium. A priori, this involves two components: the energy dissipated into the medium via the drag force (physically, this is the energy transferred to the plasma constituents through elastic collisions) and the energy taken away by the gluons from the jet which have reached a thermal distribution in momentum (since such gluons cannot be distinguished from the medium constituents anymore). As noticed at the end of Sect. 4.2.2, the drag component can be minimized by choosing $p_* = T$, so it should be enough to compute the energy carried by the thermalized part of the gluon distribution. Still, to avoid any uncertainty concerning the contribution of the drag, it is preferable to compute the energy loss as the *difference* between the original energy E of the LP and the energy carried by the jet constituents which have *not* thermalized. This definition too is a bit ambiguous though, because the distinction between thermal and non-thermal gluons is not really sharp, as already noticed. Yet, we have seen that the gluons in the tail of the distribution at $z \lesssim t - t_{\text{rel}}$ are approximately thermal, whereas those which belong to the front ($z > t - t_{\text{rel}}$) are still far away from thermal equilibrium — at least for not too late time, $t \lesssim t_{\text{br}}(E)$, when the front still exist (see e.g. Fig. 10). This observation motivates the following definition for the energy loss via thermalization:

$$\Delta E_{\text{ther}}(t) = E - \int_{t-t_{\text{rel}}}^{\infty} dz \int_{p_*}^{\infty} dp p f(t, z, p). \quad (5.6)$$

For sufficiently large times $t \gg t_{\text{br}}(E)$, all the gluons lie $z < t - t_{\text{rel}}$ (the front disappears) and $\Delta E_{\text{ther}} \simeq E$. But the most interesting situation in view of the phenomenology at the LHC, is that where the medium size L is small relative to the branching time $t_{\text{br}}(E)$ for the LP, hence ΔE_{ther} is small compared to E .

In Fig. 13 we present our numerical results for $\Delta E_{\text{ther}}(t)$ as a function of t (or, equivalently, the medium size) for the two energies of interest, $E = 25 T$ and $E = 90 T$. For comparison, we also show the corresponding prediction $\Delta E_{\text{flow}}(t)$ of Eq. (4.29); this would be the energy transferred to the medium in the ideal case where the plasma acts as a perfect absorber for the gluons with $p \lesssim T$ (without affecting the branching dynamics at $p > T$). Not surprisingly, the energy loss $\Delta E_{\text{ther}}(t)$ for the ‘physical’ cascade remains significantly lower than the ‘ideal’ expectation $\Delta E_{\text{flow}}(t)$ for all times $t \lesssim t_{\text{br}}(E)$, that is, so long as the gluon cascade has not fully thermalized. (For large times $t \gg t_{\text{br}}(E)$, these two quantities approach to each other, as they both converge towards the total energy E , as they should.) The main reason for this discrepancy is the fact that the medium is *not* a perfect sink: there is a delay in the thermalization of the soft gluons produced via branchings and, as a result, gluons with $p \sim T$ can still propagate at the speed of light over a time interval $\Delta t \gtrsim t_{\text{rel}}$ after their production.

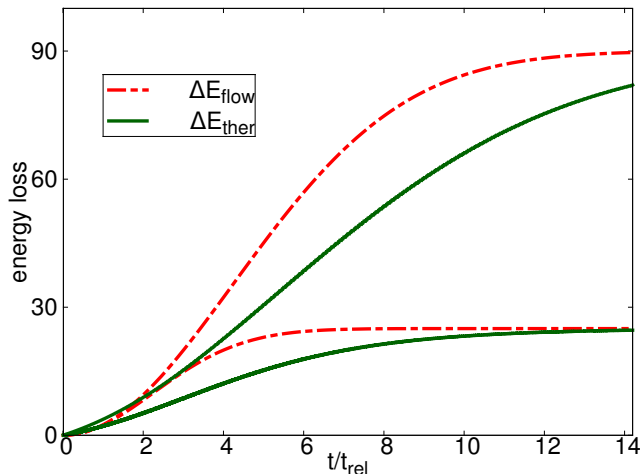


Figure 13. The energy loss towards the medium $\Delta E_{\text{ther}}(t)$ (in units of T), Eq. (5.6), plotted as a function t for $E = 25T$ and $E = 90T$. The result is compared to the flow energy (4.29) which applies to an ideal cascade.

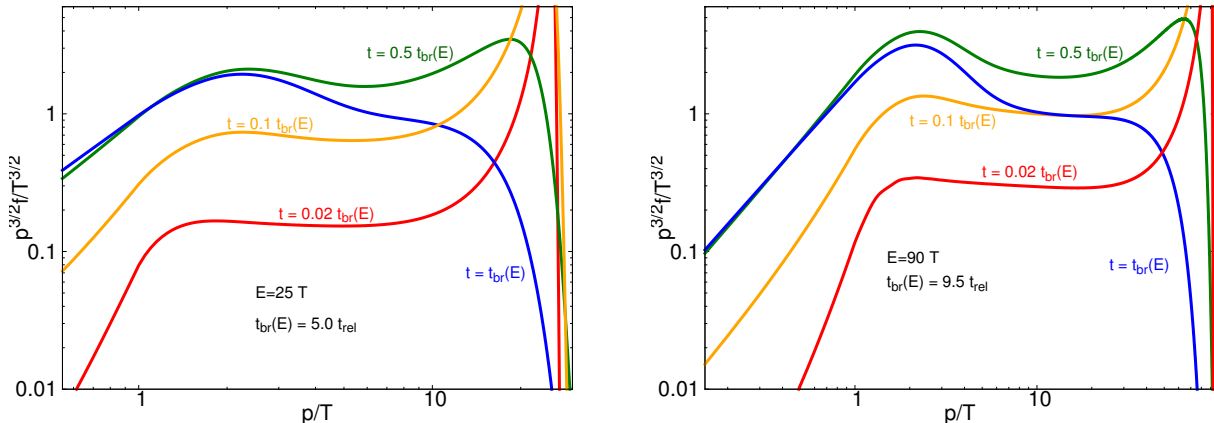


Figure 14. The gluon distribution in momentum at $t = z$ for two energies, $E = 25T$ and $E = 90T$, and for 4 values of time, which are now chosen to be the same in units of $t_{\text{br}}(E)$ for both energies. The figures show a rather broad window of approximate scaling behavior, $f \propto 1/p^{3/2}$, at not too large times $t \lesssim t_{\text{br}}(E)$.

Since the production rate increases with time, cf. Eq. (4.29), it is natural that the difference between $\Delta E_{\text{flow}}(t)$ and $\Delta E_{\text{ther}}(t)$ increases as well so long as the LP still exists, i.e. for $t \lesssim t_{\text{br}}(E)$. This trend is indeed visible in Fig. 13.

This being said, the energy loss ΔE_{ther} that we have numerically found is significantly large. By inspection of Fig. 13, we see that $\Delta E_{\text{ther}}(L) \simeq 30T$ ($= 15\text{ GeV}$) for a jet with $E = 90T$ ($= 45\text{ GeV}$) and for a medium size $L = 5 t_{\text{rel}}$ ($= 5\text{ fm}$). Furthermore, as also visible in Fig. 13, the energy loss rises quite fast with time and hence with the medium size L : at small times $t \ll t_{\text{br}}(E)$, one roughly has $\Delta E_{\text{ther}}(t) \propto t^2$, in agreement with Eq. (2.6), whereas for larger times $t \gtrsim t_{\text{br}}(E)$, $\Delta E_{\text{ther}}(t)$ approaches the total energy E of the LP: the jet is ‘fully quenched’.

Whereas the results in Fig. 13 point out towards a failure of the hypothesis of a ‘perfect sink’, this failure remains quite mild, especially at early times $t \ll t_{\text{br}}(E)$. This is already suggested by the

qualitative similarity between the gluon distribution produced by a ‘real’ jet, as shown in Fig. 8, and that generated by an ideal gluon cascade, cf. Fig. 3 and Fig. 6. To have a more quantitative test in that sense, we have studied the gluon spectrum near the front of the jet, that is, the distribution $f(t, z, p)$ produced by the kinetic equation at $z = t$. At small times $t \lesssim 0.5t_{\text{br}}(E)$, the numerical results in Fig. 14 exhibit a relatively wide window at $T < p \ll E$ where the front distribution function shows the same scaling behavior, $f(z = t, p) \propto 1/p^{3/2}$, as the ideal branching process (compare to the curved ‘w/o cutoff’ in Fig. 7). As repeatedly stressed, this scaling law is a hallmark of wave turbulence. Fig. 14 should be contrasted to the corresponding results for the spectrum $f(t, p) = \int dz f(t, z, p)$ (the curves denoted as ‘full’ in Fig. 7), which show no scaling window at all. So, in this respect at least, the gluon spectrum is potentially misleading, as anticipated in Sect. 5.2.

More generally, the ensemble of studies that we have performed in this paper demonstrate that the detailed phase-space distribution is better suited than the gluon spectrum for understanding the in-medium evolution of the jets.

6 Conclusions and perspectives

In this paper, we have presented a first study of the thermalization of the soft components of the gluon cascades generated via multiple branchings by an energetic parton which propagates through a weakly-coupled quark-gluon plasma. Our overall picture is rather simple and physically motivated, and in our opinion it is also quite robust: indeed, this picture is almost an immediate consequence of the strong separation of scales between the characteristic time for the medium-induced branchings of hard gluons and, respectively, the relaxation time for the thermalization of soft gluons. In trying to establish this picture beyond parameter estimates, we met with several difficulties and subtle points, for which we proposed at least partial solutions.

A major difficulty is the overall complexity of the problem, that we have tried to circumvent via suitable approximations, notably by carefully separating the gluons from the jet from those in the medium and by projecting the dynamics onto the one-dimensional, longitudinal, phase-space. These approximations are fully justified for the sufficiently hard gluons in the cascades, with momenta $p \gg T$, which control the dynamics of multiple branchings. On the other hand, these approximations becomes less justified when moving to the softer gluons with $p \lesssim T$, where they are at most qualitatively right. (But we have tried to carefully argue that they correctly reproduce the relevant time scales to parametric accuracy.) A particularly subtle approximation refers to the branching dynamics near the lower end of the cascades, at $p \sim T$, where we expect the cascade to terminate, on physical grounds. In our calculations, we have simply cut off the branching process at a scale $p_* \sim T$ and found that, thanks to the smearing effect of the elastic collisions, the results are not very sensitive to the precise value of this cutoff. (We have indeed checked that our numerical results remain qualitatively and even semi-quantitatively unchanged when varying this cutoff by a factor of 2 around its central value.) But it would be of course important, both conceptually and phenomenologically, to have a dynamical implementation of this cutoff, which in turn requires a consistent treatment of the full gluon distribution at soft momenta, including the inherent non-linear effects.

This discussion points towards the many ‘technical’ limitations in our approach, with potential physical consequences, which will be hopefully lifted by more detailed, future, analyses. In principle, the theoretical framework for such studies is well defined: this is set by the general kinetic equations alluded to in Sect. 3, that can be found in the literature [36, 43]. A main difficulty as compared to

previous numerical studies of such equations in the literature [39, 51, 52], is that fact that, for the jet problem at hand, one needs to explicitly deal with the strong spatial inhomogeneity introduced by the hard components of the jet.

Another interesting direction of research refers to a better understanding of the implications of the present picture for the phenomenology of jets in heavy ion collisions at RHIC and the LHC. Our first estimates for the energy loss via thermalization, which are of course very raw and must be taken with a grain of salt, are quite encouraging in that sense. In our opinion, it makes sense to compare, at least qualitatively, the quantity ΔE_{ther} introduced in Eq. (5.6) (the energy carried away by the thermalized gluons in the tail of the jet) with the energy imbalance at large angles, as measured in the context of the di-jet asymmetry. The detailed analyses of the corresponding data, notably by the CMS collaboration [20, 26], demonstrate that the energy imbalance is carried by an excess of soft hadrons ($p_T \lesssim 2$ GeV) propagating at large angles. It looks natural to associate these soft hadrons with the ‘thermalized gluons’ in our current set-up. If so, it is interesting to notice that our estimates for ΔE_{ther} in Fig. 13 are in the ballpark of 10 to 20 GeV, a value which is not unreasonable for the phenomenology alluded to above. But of course further studies, to remove some of our theoretical uncertainties and to better defines experimental observables, are still needed before aiming at a detailed comparison with the phenomenology.

Acknowledgments

We would like to thank Al Mueller for inspiring discussions during the early stages of this work and for a careful reading of the manuscript. This work is supported by the European Research Council under the Advanced Investigator Grant ERC-AD-267258 and by the Agence Nationale de la Recherche project # 11-BS04-015-01.

References

- [1] M. Gyulassy and X.-n. Wang, “Multiple Collisions and Induced Gluon Bremsstrahlung in QCD,” *Nucl. Phys.* **B420** (1994) 583–614, [arXiv:nuc1-th/9306003](#).
- [2] R. Baier, Y. L. Dokshitzer, A. H. Mueller, S. Peigne, and D. Schiff, “Radiative Energy Loss of High Energy Quarks and Gluons in a Finite-Volume Quark-Gluon Plasma,” *Nucl. Phys.* **B483** (1997) 291–320, [arXiv:hep-ph/9607355](#).
- [3] R. Baier, Y. L. Dokshitzer, A. H. Mueller, S. Peigne, and D. Schiff, “Radiative Energy Loss and P(T)-Broadening of High Energy Partons in Nuclei,” *Nucl. Phys.* **B484** (1997) 265–282, [arXiv:hep-ph/9608322](#).
- [4] B. G. Zakharov, “Fully Quantum Treatment of the Landau-Pomeranchuk-Migdal Effect in QED and QCD,” *JETP Lett.* **63** (1996) 952–957, [arXiv:hep-ph/9607440](#).
- [5] B. G. Zakharov, “Radiative Energy Loss of High Energy Quarks in Finite-Size Nuclear Matter and Quark-Gluon Plasma,” *JETP Lett.* **65** (1997) 615–620, [arXiv:hep-ph/9704255](#).
- [6] R. Baier, Y. L. Dokshitzer, A. H. Mueller, and D. Schiff, “Medium-Induced Radiative Energy Loss: Equivalence Between the Bdmps and Zakharov Formalisms,” *Nucl. Phys.* **B531** (1998) 403–425, [arXiv:hep-ph/9804212](#).
- [7] U. A. Wiedemann, “Gluon Radiation Off Hard Quarks in a Nuclear Environment: Opacity Expansion,” *Nucl. Phys.* **B588** (2000) 303–344, [arXiv:hep-ph/0005129](#).

- [8] U. A. Wiedemann, “Jet Quenching Versus Jet Enhancement: a Quantitative Study of the Bdmeps-Z Gluon Radiation Spectrum,” *Nucl. Phys.* **A690** (2001) 731–751, [arXiv:hep-ph/0008241](#).
- [9] P. B. Arnold, G. D. Moore, and L. G. Yaffe, “Photon Emission from Ultrarelativistic Plasmas,” *JHEP* **11** (2001) 057, [arXiv:hep-ph/0109064](#).
- [10] P. B. Arnold, G. D. Moore, and L. G. Yaffe, “Photon Emission from Quark Gluon Plasma: Complete Leading Order Results,” *JHEP* **12** (2001) 009, [arXiv:hep-ph/0111107](#).
- [11] P. B. Arnold, G. D. Moore, and L. G. Yaffe, “Photon and Gluon Emission in Relativistic Plasmas,” *JHEP* **06** (2002) 030, [arXiv:hep-ph/0204343](#).
- [12] R. Baier, D. Schiff, and B. Zakharov, “Energy loss in perturbative QCD,” *Ann.Rev.Nucl.Part.Sci.* **50** (2000) 37–69, [arXiv:hep-ph/0002198](#) [[hep-ph](#)].
- [13] J. Casalderrey-Solana and C. A. Salgado, “Introductory lectures on jet quenching in heavy ion collisions,” *Acta Phys. Polon.* **B38** (2007) 3731–3794, [arXiv:0712.3443](#) [[hep-ph](#)].
- [14] Y. Mehtar-Tani, J. G. Milhano, and K. Tywoniuk, “Jet physics in heavy-ion collisions,” *Int.J.Mod.Phys.* **A28** (2013) 1340013, [arXiv:1302.2579](#) [[hep-ph](#)].
- [15] D. d’Enterria, “Jet quenching,” *Landolt-Bornstein* **23** (2010) 471, [arXiv:0902.2011](#) [[nucl-ex](#)].
- [16] A. Majumder and M. Van Leeuwen, “The Theory and Phenomenology of Perturbative QCD Based Jet Quenching,” *Prog.Part.Nucl.Phys.* **A66** (2011) 41–92, [arXiv:1002.2206](#) [[hep-ph](#)].
- [17] K. M. Burke, A. Buzzatti, N. Chang, C. Gale, M. Gyulassy, *et al.*, “Extracting jet transport coefficient from jet quenching at RHIC and LHC,” *Phys.Rev.* **C90** (2014) 014909, [arXiv:1312.5003](#) [[nucl-th](#)].
- [18] G. Roland, K. Safarik, and P. Steinberg, “Heavy-ion collisions at the LHC,” *Prog.Part.Nucl.Phys.* **77** (2014) 70–127.
- [19] **Atlas Collaboration**, G. Aad *et al.*, “Observation of a Centrality-Dependent Dijet Asymmetry in Lead-Lead Collisions at $\sqrt{s_{NN}}=2.76$ TeV with the Atlas Detector at the LHC,” *Phys. Rev. Lett.* **105** (2010) 252303, [arXiv:1011.6182](#) [[hep-ex](#)].
- [20] **CMS Collaboration**, S. Chatrchyan *et al.*, “Observation and Studies of Jet Quenching in PbPb Collisions at Nucleon-Nucleon Center-Of-Mass Energy = 2.76 TeV,” *Phys. Rev.* **C84** (2011) 024906, [arXiv:1102.1957](#) [[nucl-ex](#)].
- [21] **CMS Collaboration**, S. Chatrchyan *et al.*, “Jet momentum dependence of jet quenching in PbPb collisions at $\sqrt{s_{NN}}=2.76$ TeV,” *Phys.Lett.* **B712** (2012) 176–197, [arXiv:1202.5022](#) [[nucl-ex](#)].
- [22] **ATLAS Collaboration**, G. Aad *et al.*, “Measurement of the jet radius and transverse momentum dependence of inclusive jet suppression in lead-lead collisions at $\sqrt{s_{NN}}=2.76$ TeV with the ATLAS detector,” *Phys.Lett.* **B719** (2013) 220–241, [arXiv:1208.1967](#) [[hep-ex](#)].
- [23] **CMS Collaboration**, S. Chatrchyan *et al.*, “Modification of jet shapes in PbPb collisions at $\sqrt{s_{NN}}=2.76$ TeV,” *Phys.Lett.* **B730** (2014) 243–263, [arXiv:1310.0878](#) [[nucl-ex](#)].
- [24] **CMS Collaboration**, S. Chatrchyan *et al.*, “Measurement of jet fragmentation in PbPb and pp collisions at $\sqrt{s_{NN}}=2.76$ TeV,” [arXiv:1406.0932](#) [[nucl-ex](#)].
- [25] **ATLAS Collaboration**, G. Aad *et al.*, “Measurement of inclusive jet charged-particle fragmentation functions in Pb+Pb collisions at $\sqrt{s_{NN}}=2.76$ TeV with the ATLAS detector,” [arXiv:1406.2979](#) [[hep-ex](#)].
- [26] **CMS Collaboration**, “Measurement of momentum flow relative to the dijet system in PbPb and pp collisions at $\sqrt{s_{NN}}=2.76$ TeV,” *CMS PAS HIN-14-010* (2014) .
- [27] J.-P. Blaizot, F. Dominguez, E. Iancu, and Y. Mehtar-Tani, “Medium-induced gluon branching,” *JHEP*

- 1301** (2013) 143, [arXiv:1209.4585 \[hep-ph\]](#).
- [28] J.-P. Blaizot, E. Iancu, and Y. Mehtar-Tani, “Medium-induced QCD cascade: democratic branching and wave turbulence,” *Phys.Rev.Lett.* **111** (2013) 052001, [arXiv:1301.6102 \[hep-ph\]](#).
- [29] J.-P. Blaizot, F. Dominguez, E. Iancu, and Y. Mehtar-Tani, “Probabilistic picture for medium-induced jet evolution,” *JHEP* **1406** (2014) 075, [arXiv:1311.5823 \[hep-ph\]](#).
- [30] L. Fister and E. Iancu, “Medium-induced jet evolution: wave turbulence and energy loss,” [arXiv:1409.2010 \[hep-ph\]](#).
- [31] A. Kurkela and U. A. Wiedemann, “Picturing perturbative parton cascades in QCD matter,” *Phys.Lett.* **B740** (2015) 172–178, [arXiv:1407.0293 \[hep-ph\]](#).
- [32] J.-P. Blaizot, Y. Mehtar-Tani, and M. A. C. Torres, “Angular structure of the in-medium QCD cascade,” *Phys.Rev.Lett.* **114** no. 22, (2015) 222002, [arXiv:1407.0326 \[hep-ph\]](#).
- [33] L. Apolinário, N. Armesto, J. G. Milhano, and C. A. Salgado, “Medium-induced gluon radiation and colour decoherence beyond the soft approximation,” *JHEP* **1502** (2015) 119, [arXiv:1407.0599 \[hep-ph\]](#).
- [34] J.-P. Blaizot, L. Fister, and Y. Mehtar-Tani, “Angular distribution of medium-induced QCD cascades,” *Nucl.Phys.* **A940** (2015) 67–88, [arXiv:1409.6202 \[hep-ph\]](#).
- [35] J.-P. Blaizot and Y. Mehtar-Tani, “Energy flow along the medium-induced parton cascade,” [arXiv:1501.03443 \[hep-ph\]](#).
- [36] R. Baier, A. H. Mueller, D. Schiff, and D. Son, “‘Bottom up’ thermalization in heavy ion collisions,” *Phys.Lett.* **B502** (2001) 51–58, [arXiv:hep-ph/0009237 \[hep-ph\]](#).
- [37] R. Baier, Y. L. Dokshitzer, A. H. Mueller, and D. Schiff, “Quenching of hadron spectra in media,” *JHEP* **0109** (2001) 033, [arXiv:hep-ph/0106347 \[hep-ph\]](#).
- [38] S. Jeon and G. D. Moore, “Energy loss of leading partons in a thermal QCD medium,” *Phys.Rev.* **C71** (2005) 034901, [arXiv:hep-ph/0309332 \[hep-ph\]](#).
- [39] B. Schenke, C. Gale, and S. Jeon, “Martini: an Event Generator for Relativistic Heavy-Ion Collisions,” *Phys. Rev.* **C80** (2009) 054913, [arXiv:0909.2037 \[hep-ph\]](#).
- [40] J.-P. Blaizot and Y. Mehtar-Tani, “Jet Structure in Heavy Ion Collisions,” [arXiv:1503.05958 \[hep-ph\]](#).
- [41] V. Zakharov, V. Lvov, and G. Falkovich, “Kolmogorov spectra of turbulence, Volume 1,” *Springer-Verlag* (1992) 264 p.
- [42] S. Nazarenko, “Wave Turbulence,” *Springer-Verlag, Berlin* (2011) 279 p.
- [43] P. B. Arnold, G. D. Moore, and L. G. Yaffe, “Effective kinetic theory for high temperature gauge theories,” *JHEP* **0301** (2003) 030, [arXiv:hep-ph/0209353 \[hep-ph\]](#).
- [44] E. Lifshitz and L. Pitaevskii, “Physical Kinetics,” (Pergamon Press, New York, 1981).
- [45] G. D. Moore and D. Teaney, “How much do heavy quarks thermalize in a heavy ion collision?,” *Phys.Rev.* **C71** (2005) 064904, [arXiv:hep-ph/0412346 \[hep-ph\]](#).
- [46] R. Rapp and H. van Hees, “Heavy Quarks in the Quark-Gluon Plasma,” [arXiv:0903.1096 \[hep-ph\]](#).
- [47] J. Ghiglieri and D. Teaney, “Parton energy loss and momentum broadening at NLO in high temperature QCD plasmas,” [arXiv:1502.03730 \[hep-ph\]](#).
- [48] A. Kurkela and G. D. Moore, “Thermalization in Weakly Coupled Nonabelian Plasmas,” *JHEP* **1112** (2011) 044, [arXiv:1107.5050 \[hep-ph\]](#).
- [49] J.-P. Blaizot, B. Wu, and L. Yan, “Quark production, Bose-Einstein condensates and thermalization of

- the quark-gluon plasma,” *Nucl.Phys.* **A930** (2014) 139–162, [arXiv:1402.5049 \[hep-ph\]](#).
- [50] P. B. Arnold, G. D. Moore, and L. G. Yaffe, “Transport coefficients in high temperature gauge theories. 2. Beyond leading log,” *JHEP* **0305** (2003) 051, [arXiv:hep-ph/0302165 \[hep-ph\]](#).
- [51] A. Kurkela and E. Lu, “Approach to Equilibrium in Weakly Coupled Non-Abelian Plasmas,” *Phys.Rev.Lett.* **113** no. 18, (2014) 182301, [arXiv:1405.6318 \[hep-ph\]](#).
- [52] A. Kurkela and Y. Zhu, “Isotropization and hydrodynamization in weakly coupled heavy-ion collisions,” [arXiv:1506.06647 \[hep-ph\]](#).
- [53] X.-G. Huang and J. Liao, “Kinetic evolution of the glasma and thermalization in heavy ion collisions,” *Int.J.Mod.Phys.* **E23** (2014) 1430003, [arXiv:1402.5578 \[nucl-th\]](#).
- [54] P. B. Arnold, “Simple Formula for High-Energy Gluon Bremsstrahlung in a Finite, Expanding Medium,” *Phys. Rev.* **D79** (2009) 065025, [arXiv:0808.2767 \[hep-ph\]](#).
- [55] P. B. Arnold and W. Xiao, “High-energy jet quenching in weakly-coupled quark-gluon plasmas,” *Phys.Rev.* **D78** (2008) 125008, [arXiv:0810.1026 \[hep-ph\]](#).